Journal of Energy Storage 96 (2024) 112605

Contents lists available at ScienceDirect

Journal of Energy Storage

journal homepage: www.elsevier.com/locate/est

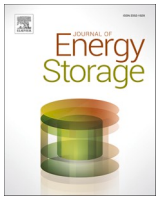

Review Article

Research trends in electrospun conducting polymers derived CNFs and their composite as the potential electrodes for high-performance flexible supercapacitors

Jining Lin [a,1], K. Karuppasamy [b,c,1], Ranjith Bose [b,c], Dhanasekaran Vikraman [d], Saeed Alameri [c,e], T. Maiyalagan [f], Hyun-Seok Kim [d], Akram Alfantazi [b,c,*], Jan G. Korvink [a], Bharat Sharma [a,**]

[a] Institute of Microstructure Technology, Karlsruhe Institute of Technology, Hermonn-Von-Helmholtz-Platz 1, 76344 Eggenstein-Leopoldshafen, Germany
[b] Department of Chemical and Petroleum Engineering, Khalifa University of Science and Technology, Abu Dhabi 127788, United Arab Emirates
[c] Emirates Nuclear Technology Center (ENTC), Khalifa University of Science and Technology, Abu Dhabi 127788, United Arab Emirates
[d] Division of Electronics and Electrical Engineering, Dongguk University-Seoul, Seoul 04620, Republic of Korea
[e] Department of Mechanical and Nuclear Engineering, Khalifa University of Science and Technology, Abu Dhabi 127788, United Arab Emirates
[f] Department of Chemistry, SRM Institute of Science and Technology, Kattankulathur 603203, Tamil Nadu, India

ARTICLE INFO

Keywords:
Electrospinning
Carbon nanofibers
Composites
Conducting polymers
Wearable electronic devices

ABSTRACT

Electrochemical energy storage (EES) devices are much needed due to their improved reliability and sustainability. As a class of EES, supercapacitors (SCs) have exhibited relatively more advantages, including high power density, longer cycle life, rapid charge-discharge speed, and high energy efficiency. Carbon materials are the electrodes of most significant concern in high-performance SCs. Among the carbon materials, the electrospun-derived carbon nanofibers (CNFs) and their composites are of high interest due to their scalable preparative process, high specific surface area (SSA), and porosity, and apt to construct essentially conducting self-standing electrodes for EES devices leading to improved electrochemical performance and energy storage capacitance. Conducting polymers (CPs)-based materials can be used as SCs' electrodes due to their versatility, supreme conductivity, redox property, inherent elasticity, low cost, and facile production. This review aims to provide a precise overview of the recent trends in CPs, especially concentrating on polyaniline (PANI), polythiophene (PTh), polypyrrole (PPy), and poly (3,4-ethylene dioxythiophene) (PEDOT) based electrospun CNFs and their composite as the potential electrodes for high-performance flexible SCs. The review systematically addresses synthesis techniques, design concepts, recent progress, challenges, and future perspectives on developing binder-free, self-standing CPs-derived CNFs/composites-based electrodes for constructing future flexible SCs.

1. Introduction

The evolution of portable, flexible, and wearable electronic systems has motivated research on fabrication processes, control of nano-structured morphology, and improved materials to attain affordable green and renewable electrochemical energy storage (EES) systems [1–4]. The 21st-century world is incomplete without wearable, smart, and portable electronic devices. For example, smartphones with various critical applications and functions, such as healthcare, implantable medical devices, activity trackers, sensors, smart watches, etc., have made daily routines more convenient [5–7]. Indeed, the excess energy consumption of these smart electronic devices requires highly efficient EES systems, and the rapid extraction and consumption of fossil fuels through combustion processes, the significant adverse effects and destructions on the global environment and economics in the coming future are gaining more and more focus [8–11]. Thus, the depreciation

* Correspondence to: A. Alfantazi, Department of Chemical and Petroleum Engineering, Khalifa University of Science and Technology, Abu Dhabi 127788, United Arab Emirates.
** Corresponding author.
E-mail addresses: akram.alfantazi@ku.ac.ae (A. Alfantazi), bharat.sharma@kit.edu (B. Sharma).
[1] Jining Lin (J. L) and K. Karuppasamy (K. K) contributed equally to this work.

https://doi.org/10.1016/j.est.2024.112605
Received 1 April 2024; Received in revised form 11 June 2024; Accepted 16 June 2024
Available online 28 June 2024

of energy efficiency and the pursuit of renewable and environmentally friendly energy sources as alternatives to fossil fuels are considered excellent promotions for the sustainable development of our economy and society [12]. EES systems, encompassing fuel cells, batteries, and electrochemical capacitors, are increasingly influencing our daily existence [13–16]. Owing to their promising performances, such as highly rapid discharge/charge rates and high-power densities, electrochemical capacitors or SCs have become one of the most attractive alternatives to batteries and other energy storage technologies in the transportation and electronics industries [17–20]. Further, it has a more significant energy density than conventional SCs, longer cycle life, and higher power density than traditional secondary batteries. SCs comprise various passive and active components. In most studied or reported SCs, the passive yet essential elements are the separators, substrates, packaging compounds, and binders [18,21]. Among these passive components, two main components, including the separator and binder, could be easily removed by constructing an electro-spun polymer-derived self-standing nanofiber electrode material.

The well-ordered nanostructured materials contain specific functional behaviors with excellent stability; hence, they can be widely employed in drug delivery and tissue engineering, batteries, SCs, photovoltaics, photonic devices, water splitting and catalysis, etc. [21–23]. To date, various fabrication technologies, including hydrothermal, sol-gel, template, co-precipitation, and successive ionic-layer adsorption and reaction, etc. have been investigated to construct multiple forms (1D, 2D, and 3D) of nanostructures, including nanotubes, nanoflowers, nanorods, and nanowires, etc. On the other hand, electrospinning and electro-spraying are vastly employed in various research areas, including material science, tissue engineering, drug delivery, and nanotechnology [24]. Both techniques use an electric field to generate charged droplets or fibers from a liquid solution or melt. Electrospinning offers a straightforward approach to creating nanofibers, mats (webs), yarns, and more [25–27]. The resulting nanofibrous material's final structure, functionality, and morphology are significantly influenced by the polymer's inherent characteristics, the solvent's inherent characteristics, and the specific parameters used during processing. This technique enables the production of continuous fibers with diameters ranging from nano to microscale [28–30]. In recent times, the needle and needleless-related electrospinning processes have become more valiant for the functionalization of electrodes and supports, which could be achieved with the help of another physical process, such as magnetic-field electrospinning and co-axial electrospinning processes [31,32]. Henceforth, it can be widely used to construct nanofibers for various applications, including sensors, dental, air and water filtration, cosmetics, energy, tissue grafts, and acoustics [28,33].

Carbon materials, including carbon nanotubes, graphene (GE), carbon nanofibers (CNFs), reduced graphene oxide (RGO), and activated carbon (AC), are the most vastly concerned electrodes in the SCs application. It is well known that the electrospinning process-assisted polymer-derived self-standing electrodes are generally flexible. Carbonized polymer fibers are a widely investigated electrode material for SCs due to their high specific surface area (SSA), good chemical stability, and excellent electrical conductivities [33–37]. In addition, they can function as conductive additives, templates for supporting pseudo-capacitive metal oxide/chalcogenide, and electrode materials in EES devices. The CNFs derived by the carbonization of electro-spun polymer fibers have excellent inherent physicochemical and textural properties; henceforth, they could contribute majorly to the electrochemical double-layer capacitance (EDLC). Non-self-standing electrode materials use nickel foam and aluminum/copper foils as substrates that do not give charge storage characteristics [38]. In such cases, the active electrode materials are coated over the substrates using polymer binders like polyvinylpyrrolidone (PVP), polyvinylidene fluoride (PVDF), and polyvinylidene fluoride hexafluoropropylene (PVdF-*co*-HFP), which are highly intolerant for the storage properties [23]. Compared to the conventional binder-based coating process of electrode materials, it is essential to account that various pseudo-capacitive materials (metal oxides/chalcogenides) can be directly grown over the electro-spun derived polymer fiber and CNFs through hydrothermal and electrodeposition techniques without the use of binders [22]. Compared to other carbon allotropes, CNFs possess very low crystallinity and may comprise many defects and functional moieties, leading to better electrochemical performance in storage devices. CNFs have relatively lower electrical conductivity and SSA than carbon nanotubes (CNTs), but the fabrication cost and facile dispersion behaviors make them more special than other carbon materials. Hence, they could be employed mainly in energy storage materials and polymer nanocomposites' reinforcement [22,39,40].

Electrospinning (ES) is the most versatile and adaptable process that permits one to design and develop new morphologies, including porous fibers, core-shell hollow fibers, etc., [41–43]. Moreover, the carbonization of fibers after the ES process could be supported to graft various nanostructured compounds, including carbon nanotubes (CNTs), GE, and MOFs over CNFs, effectively employed as the binder-free energy storage electrodes. Introducing heteroatoms (S, N, and F) into CNF's matrix could improve the electrochemical storage properties of the CNFs. This could be achieved by calcinating the CNFs in sulfur or nitrogen atmospheres or using external additives like thiourea or urea [40]. The heteroatoms-modified CNFs could extend the interlayer distance, creating extra reactive sites, thus enhancing the overall electrical conductivity. One of the significant beneficial properties of these electro-spun fibers (CNFs and heteroatom-doped CNFs) is that they do not need any support or favor from the substrate (current collector) to migrate electrons. Further, these CNFs hold pseudo-capacitive compounds within and over them and function as the current collector [44]. Interestingly, it is essential to understand that these CNFs or their composite could significantly increase the storage characteristics of electrodes via the EDLC behavior of CNFs and the pseudocapacitance behavior of heteroatoms or metal oxides/chalcogenides. As stated earlier, other advantageous properties of CNFs, such as high SSA and porosity, excellent conductivity, lightweight and self-standing nature, etc., have made these materials the unavoidable candidates for high-performance SCs intended for use in flexible wearable electronic devices [22,45].

To date, quite a handful of reports on electrospun-derived nanofibers for electrochemical energy storage devices have been reported [33,40,45]. Recently, the electrospun-derived CNFs, CNF composites, and carbon-free metal oxide electrodes for SCs were elaborated on and reported elsewhere [46]. The utilization of lignin-based electrospun CNFs in EES devices has been reported by Ma and his coworkers [47]. Roy et al. have recently reviewed the graphitic carbonitride electrospun-assisted flexible, free-standing electrodes for wearable electronic devices [48]. Though these studies, as stated above, talk over electrospun fibers, these articles significantly highlight binder-based electrodes, etching/doping, Mo-based composite fibers, metal-oxide-free carbon compounds, etc. [22,28,33,40,49,50]. Nevertheless, a detailed review of electrospun CPs such as polyaniline (PANI), polythiophene (PTh), and polypyrrole (PPy) derived CNFs, and their composites as the binder-free innovative electrodes aimed at flexible SCs application is still not yet reported in detail till date. Compared to pristine electrospun CNFs, CPs-derived electrospun CNFs have offered excellent electrical conductivity, surface chemistry, and flexibility [51]. The CPs-derived electrospun CNFs further provide improved interfacial characteristics in the resultant CNFs, which enhance compatibility and adhesion. Further, these CPs-based electrospun CNFs offer excellent porous properties with a large surface area, facilitating ions transport and improving the overall electrochemical performance [52]. These advantageous characteristics show a potential foundation for constructing new electrode materials with desirable qualities for various applications in EES, electronics, biomedical, and sensor fields [53]. Henceforth, an extensive review of research on conducting polymers-based electrospun, binder-free, self-standing CNFs for high-energy SCs is essential to identify their practical

viability at this juncture.

Based on this idea, this current review's ultimate and prime focus is to highlight the recent state-of-the-art preparative process and recent progress in conducting polymers-based electrospun CNFs and their composites for flexible, high-energy SCs. Also, in this review, we debate the fabrication strategy and principle of the ES process, the optimal experimental parameters of various CPs, and their composites for high-performance SCs. In the end, an outlook and overview of the future direction and advancement status of mixed CPs-based CNFs and their composites are elaborated.

2. Key parameters in controlling the formation of fibers

Interestingly, the concentration of the polymer solution plays a crucial role in determining the structures of the materials produced through the ES process. Specifically, in ES, an increase in solution concentration leads to a corresponding increase in solution viscosity, which results in the formation of thicker and more uniform fibers, as demonstrated in Fig. 1(a–h) [54,55]. As evident from the Figure, spherical particles are observed at lower concentrations. When the attention nears a critical point, bead-on-string morphologies often emerge, characterized by electrospun fibers displaying bead-like structures. Beyond this crucial solution concentration, uniform fibers can be formed. Furthermore, the surface tension of the solution also increases with an increase in solution concentration, leading to a reduction in fiber diameter [56,57]. Hence, a higher solution concentration during ES produces thinner and more uniform fibers, as shown in Fig. 1(a–h). Further, the shear viscosity has been compared with the morphology regimes, especially in determining the difference in slope values of the concentration vs relative viscosity plot, as displayed in Fig. 1(i) [58]. It is evident from the plot that the concentration changes of the entangled regime at the start, and then the critical entanglement concentration and fiber formation concentration could be identified as being in a heavily entangled regime. Based on the entanglement concentration, the morphology varies from beads to beads-on string and finally into fiber formation, as indicated in Fig. 1(i). The critical entanglement value is 1.7-25× for the proposed concentrations of all polymer hosts, consistent with the literature [42,59].

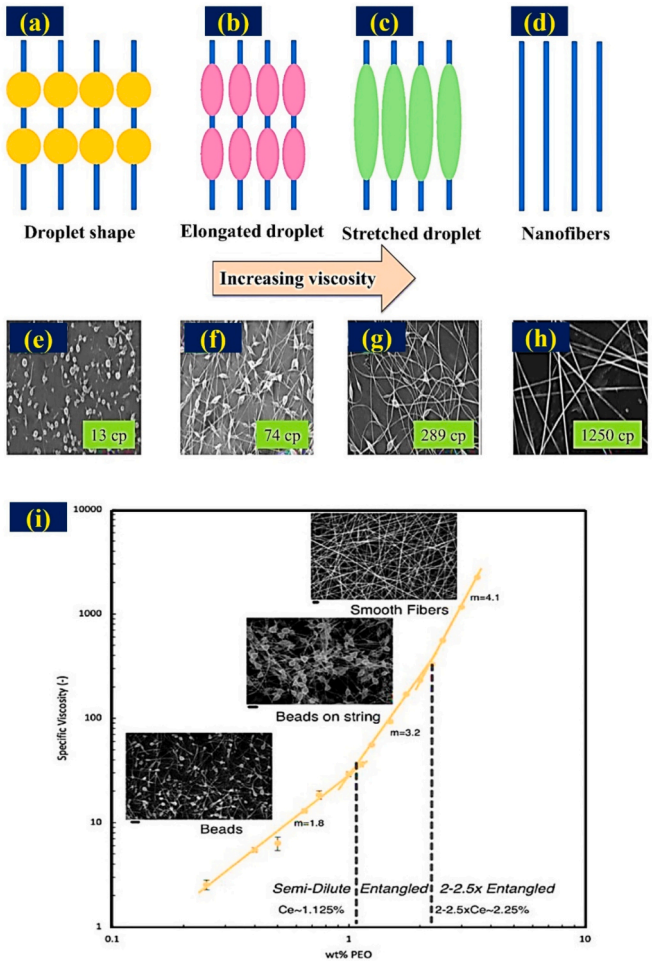

Fig. 1. (a–d) Typical representation of the influence of polymer solution viscosity enhancement on the morphological features of electrospun CNFs, reproduced with permission from Ref [63], (e–h) the morphological characteristics of various beaded fibers as a function of solution viscosity under the electric field of 0.7 kV cm^{-1}, the boundary of each picture is around 20 μm long, reproduced with permission from Ref [55], (i) specific viscosity as the function of PEO/H_2O mixture concentration displaying three regimes with their respective electrospun morphologies, reproduced with permission from Ref [58].

The voltage applied between the spinneret and the collector affects the stretching and elongation of the polymer jet during the ES process. Increasing the applied voltage enhances the electric field strength, leading to increased elongation and decreased fiber diameter. However, excessively high voltages can cause instability in the jet, resulting in beading or the formation of irregular fibers. Therefore, finding an appropriate voltage range is crucial to achieving the desired fiber morphology and quality [60]. The distance between the spinneret and the collector (target) affects the trajectory and solidification of the electrospun fibers. This parameter influences the flight time and evaporation of the solvent or carrier liquid from the polymer jet before it reaches the collector. Increasing the distance generally allows for more solvent evaporation, leading to longer flight times and increased fiber alignment. However, if the distance is too large, the fibers may become misaligned or form a non-uniform mat. Therefore, optimizing the distance is necessary to control the alignment and density of the electrospun fibers [60]. The polymer or precursor solution's flow rate determines the material delivered to the spinneret during ES. Higher flow rates tend to result in thicker fibers due to increased polymer concentration in the jet. Conversely, lower flow rates can lead to thinner fibers. Additionally, the flow rate influences the fiber morphology, as high flow rates may cause the formation of beads or irregular fibers. Therefore, finding an appropriate flow rate is essential for obtaining uniform and desired fiber characteristics [61,62].

3. Conducting polymers-based CNFs for SCs

Materials for flexible electrodes have garnered significant interest due to their high demand in energy storage devices, particularly in SCs that power a wide range of flexible and wearable electronic systems. Generally, based on their charge storage mechanisms, the materials used in SCs electrodes can be divided into two categories: i) Carbon-based materials and their derivatives used in electric double-layer capacitors (EDLCs), such as activated carbon (AC), porous carbon, carbon nanotubes (CNTs), GE, carbon nanofibers (CNFs), and others [64–70]; ii) Metal oxides/nitrides/sulfides and conducting polymers, including PANI and PPy, are used as PC electrodes [71–73]. Conventional conducting polymers, such as PANI with a capacitance of 1284 F g^{-1}, PPy with a capacitance of 480 F g^{-1}, PTh with a capacitance of 250 F g^{-1}, and their byproducts, have been employed as the promising pseudocapacitive electrode materials for SCs [68,74,75]. PPy and PANI exist in a p-doped state because the reduction potential of the electrolytes used is greater than the n-doping potential. On the other hand, PTh and its derivatives can exhibit both p-doping and n-doping behavior [68].

3.1. Polypyrrole (PPy) fibers

Conducting polymer PPy has garnered notable interest recently due to its distinctive attributes and promising potential across diverse

sectors. It is a type of organic polymer synthesized by the oxidative polymerization of pyrrole monomers. PPy has a highly conjugated structure with alternating single and double bonds, which gives electrical conductivity. It is known for its high degree of flexibility, which makes it a desirable material for various applications, primarily in flexible SCs, as shown in Fig. 2(a). It can synthesized in two ways, either by chemical oxidative polymerization or interfacial polymerization [76]. The typical chemical oxidative polymerization using the initiator 2,4-diamino diphenylamine, $FeCl_3$ under various acids (camphor sulfonic acid, HNO_3, $HClO_4$, and HCl) as the solvent media to form PPy nanosphere is represented in Fig. 2(b). The corresponding FE-SEM images using these acids are displayed in Fig. 2(c–f). Based on the morphological analysis, it is confirmed that the diameter of PPy nanospheres could be tuned based on different doping acids. The average diameter of PPy nanospheres using camphor sulfonic acid, HNO_3, $HClO_4$, and HCl were found to be 220, 200, 110, and 85 nm, respectively. Despite its relatively high mass density, this phenomenal attribute sets PPy apart from other conducting polymers [77]. PPy can be doped with various ions, including Cl^-, I^-, and Br^-, to enhance its conductivity (Fig. 2(b)). For example, PPy doped with Cl^- counter-ions exhibited distinct cyclic voltammetry (CV) curve shapes when using different electrolyte solutions, one containing univalent anions (Cl^-) and bivalent cations (Mg^{2+} and Ca^{2+}), and the other containing univalent cations (Na^+) and bivalent or large anions (CO_3^{2-} and SO_4^{2-}). This phenomenon indicates that replacing counter-ions in the polymer matrix with bivalent or large anions is not feasible [78]. One of the most attractive properties of PPy is its ability to change its electrical conductivity in response to external stimuli, such as temperature, pH, and light. This makes it a promising material for use in sensors and actuators. PPy is a good electrode material for SCs due to its high surface-to-volume ratio and ease of adaptability to various forms and structures. Furthermore, by combining PPy with other nanostructured materials such as GE and CNTs, the charge storage capacity of the resulting PPy nanocomposite can be significantly improved due to increased contact SSA and enhanced ion diffusion rate [43,79,80]. Therefore, optimization of the counter-ion valence and the ion valences in the electrolyte solution can improve the electrochemical performance of SCs. However, it is essential to note that the performance of SCs predominantly relies on the electrodes, specifically on the active materials immobilized on the electrode surfaces [81]. The benefits of PPy render it a promising option for creating lightweight, high-performance SCs that can be easily adapted for portable and flexible electronic power sources. This application has been a particularly active area of research in the energy storage field of late.

Due to its large SSA, a planar electrode has emerged as a promising candidate for high-performance SCs. Moreover, incorporating a flexible substrate allows the electrode to be bendable or twistable, aligning with the need for adaptable energy storage approaches. Several studies have investigated nanostructured PPy and its composites as materials for this electrode type. As an example, an advanced core-shell nanoarray comprising a PPy core and a shell composed of layered double hydroxides (LDHs) has been electrodeposited onto a nickel form using a two-step procedure [82]. Functioning as a flexible electrode in high-performance SCs, this nanoarray utilizes its inner PPy core nanoarrays to serve as a current collector, thus bolstering conductivity. Simultaneously, the outer LDH layer acts as a safeguard, curbing the potential metric expansion and contraction of PPy over extended cycling periods. The distinctive core-shell architecture yields an impressive specific capacitance of 2342 F g^{-1}. Furthermore, an in-situ approach has synthesized an autonomously assembled hybrid film comprising single-wall carbon nanotubes (SWCNTs), MnO_2, and PPy [83]. Enhancing conductivity, ion diffusion rate, and charge-transfer resistance, the binder-free electrode, comprising layers of SWCNT and PPy, achieves a specific capacity of 351 F g^{-1} relative to the overall electrode weight. This translates to an energy density of 39.7 Wh kg^{-1} and a power density of 10 kW kg^{-1}. With its exceptional flexibility, this planar electrode is ideally suited for portable device applications [84].

This section briefs the various carbon compounds such as RGO, GE, and CNT incorporated over the electrospun CNFs/PPy electrodes. For instance, core-shell structured CNFs have been constructed by Chen et al. through the carbonization of electrospun PAN nanofibers [85]. The obtained core-shell CNFs were further conductively modified by electrodepositing PPy and RGO over its surface (CNFs-yarn@PPy@RGO) and employed as the potential electrode material for fiber-structured

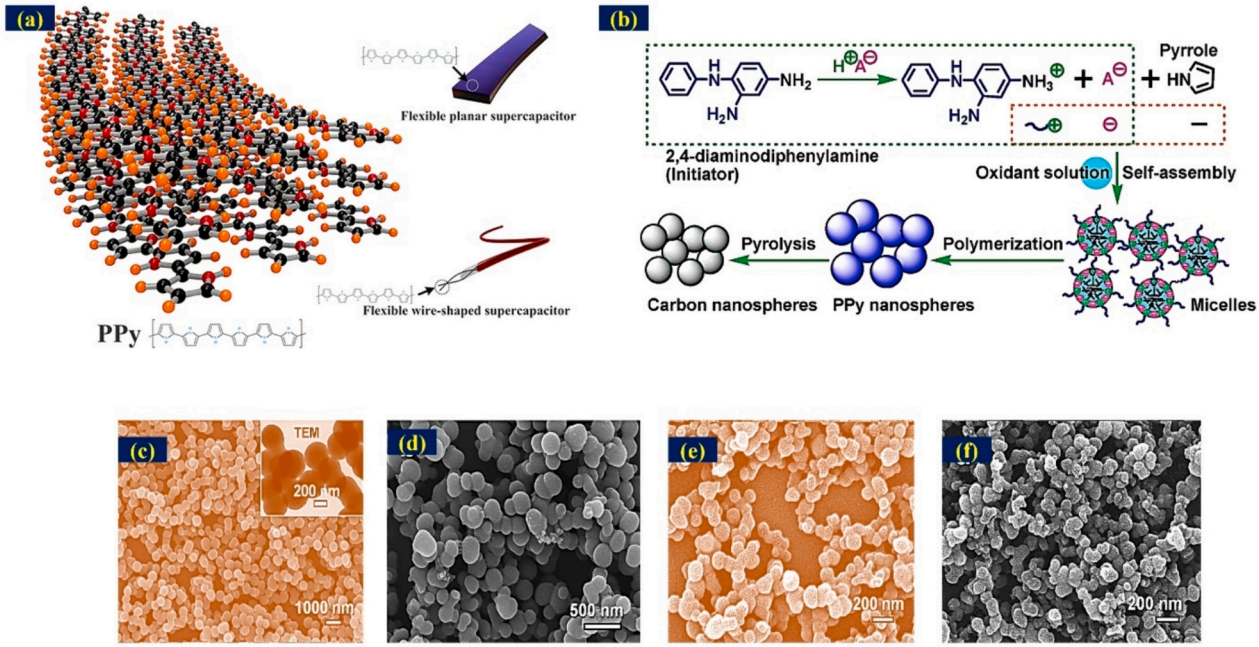

Fig. 2. (a) Typical representation of PPy-based flexible SCs, reproduced with permission from Ref [76], (b) schematic representation for the formation mechanism of PPy-based carbon nanospheres, (c–e) their corresponding FE-SEM images of PPy-based carbon nanospheres (NSs) using different acids including (c) chlorosulfonic acid, (d) perchloric acid, (e) nitric acid and (f) HCl with the initiator 2,4-diamino phenylamine (10 mol%), reproduced with permission from Ref [77].

solid-state SCs. The schematic representation for the preparative process is sketched in Fig. 3(a). They have observed that the uniform coating of RGO over CNFs-yarn@PPy might be attributed to the pi-pi interactions. Also, the prepared CNFs has an outstanding SSA of 137.5 $m^2 g^{-1}$ with a mean pore size of ~2.5 nm. The same pristine CNFs-yarn electrode exhibits excellent electrochemical behavior and is stable over 10,000 GCD cycles, as demonstrated in Fig. 3(b–d). Based on the CV, an EDLC behavior with a potential window of 1 V has been observed. The highest capacitance of 30.4 F g^{-1} with excellent durability over 10,000 cycles has been recorded for the CNFs-yarn electrode. After incorporating the PPy, the average fiber diameter is around 400 μm. When these electrodes are subjected to electrochemical analyses using PVA/H_3PO_4 electrolyte, they show outstanding EDLC capacitive performance and excellent retention behavior. The highest capacitance achieved for the proposed electrode is 92.5 F g^{-1}, which might be credited to the components' core-shell structure and synergistic behavior.

Using PAN fibers, the same research team further investigated a binder-free, flexible electrode comprised of CNFs@PPy@RGO for the flexible solid-state SCs [86]. The electrode's capacitance improved further in the PVA/H_2SO_4 gel electrolyte medium for the prepared flexible device and achieved a maximum of 188 F g^{-1}. In brief, they constructed the flexible solid-state SCs device with two pieces of CNFs@PPy@RGO electrode with the size of 1 × 2 cm, followed by the coating of gel electrolyte over the electrode and afterward sealed in a polyethylene terephthalate (PET) film. When these two electrode devices are subjected to CV analysis at different scan rates, they show an EDLC behavior with a shaped curve in the voltage range of −0.2 V to 0.8 V, as depicted in Fig. 3(e). Based on the integral area of the CV curve, its corresponding capacitance has been found, and the maximum of 188 F g^{-1} at 2 mV s^{-1} has been obtained (Fig. 3(f)). In addition, it has stable over 10,000 charge-discharge cycles with a retention of 59.5 %, as depicted in Fig. 3(g). Interestingly, they further checked the flexibility of the two-electrode device at different bending angles such as 0, 30, 60, and 90° and studied their corresponding electrochemical behavior as demonstrated in Fig. 3(h–k). As shown in Fig. 3(h–j), they have found that the similar CV fashion at various bending angles confirms its excellent flexibility. When these three flexible SCs are connected in series, they can light a red LED with a voltage of 2.5 V, as given in Fig. 3(k), confirming its practical viability. This scalable and facile process of preparing electrodes paves the way for their use as promising candidates in high-performance flexible SCs. Later, Mahore et al. developed a similar electrode system comprising electrospun nanofibers from PPy/CNT/MnO_2 composite and reported elsewhere for its excellent electrochemical activity [87].

Sung and coworkers have innovatively applied the electropolymerization technique to fabricate the PPy decored CNFs (CNFs@PPy), marking a significant advancement in the field of flexible SCs [88]. The study meticulously examined the role of various experimental conditions, such as the supporting electrolyte, time, electropolymerization system design, applied current, and electrolyte concentration, to achieve and assemble highly efficient flexible SCs with exceptional EES electrodes based on PPy. The authors further studied the influence of the electropolymerization applied current on the morphology of PPy and the electrochemical characteristics of CNFs@PPy. Fig. 4(a–c) illustrates the low-magnification FE-SEM images of synthesized CNFs@PPy at the applied current of 10, 30, and 50 mA, respectively. Because of the similar electropolymerization time, the high applied potential is expected to create many holes in the electropolymerization process. In addition, the thickness of PPy over CNFs increases with an increase in applied current, which is visible in the high magnification FE-SEM micrographs, as displayed in Fig. 4(d–f). It is interesting to note that the thickness of PPy was small at the low applied current (10 mV) and vice versa at the high applied current of 50 mV. Also, few particle-like structures are unseen at high applied currents, indicating that the PPy are unevenly distributed over the CNFs' surface at high applied currents. The particle-like structure vanishing for the CF@PPy at high applied currents might be attributed to the large charge density in the voids between the particle-like structures. This process leads to filling the gaps and to the CNFs@PPy flatter surface. The authors constructed the flexible SCs using two symmetrical CNFs@PPy and PVA/H_3PO_4 gel polymer electrolyte. The assembled cell delivered the appropriate capacitance of 30 F g^{-1} at 0.1 A g^{-1} with a capacitance retention of 70 %. This proposed method gives a facile, time-saving protocol for synthesizing CPs-based flexible SCs.

Similarly, Wang and team developed two-step fabrication processes, including ES and electropolymerization, to construct PPy@PAN@ cotton yarn electrodes and employed them in high-performance flexible SCs [89]. The authors further studied the influence of the PPy concentration on the morphology of PAN@cotton yarn and the electrochemical characteristics of PPy@PAN@cotton yarn electrode. Fig. 4(g–l) illustrates the pristine PAN/cotton yarn and various concentrations (0.1 M to 0.5 M) of PPy monomer incorporated PAN@cotton yarn electrodes. It is evident from the micrographs that the PPy deposited on the yarn surface differs with the concentration of PPy, i.e., as the concentration of pyrrole monomer increases, the deposited amount of PPY over the yarn increases. When the concentrations were less than 0.3 M (Fig. 4(h–j)), the PPy was attached to the yarn surface in a dispersed manner. At the concentration of 0.4 M, the PPy was uniformly distributed over the yarn surface, as shown in Fig. 4(k). When the concentration of PPy increases beyond 0.4 M, the agglomeration effect happens on the yarn's surface, as shown in Fig. 4(l). Based on these morphological results, the authors confirmed the optimized concentration of pyrrole monomer as 0.4 M. The resultant electrode delivered the maximum areal capacitance of 37.6 F cm^{-3} at 0.87 mA cm^{-2}. The flexible SCs further provided outstanding energy and power densities of 0.047 mWh cm^{-2} and 4.32 mW cm^{-2}, suggesting their wide uses in wearable smart textiles.

Incorporating PPy into CNFs increases the active SSA and enhances the accessibility of the electrode material for electrolyte ions. This leads to improved charge storage capacity and specific capacitance. PPy's redox properties contribute to the overall capacitance enhancement, as the redox reactions occurring at the PPy/electrolyte interface provide additional pseudocapacitance contributions. The unique combination of PPy's high pseudocapacitance and CNF's high electrical conductivity produces enhanced power and energy densities for SCs. The rapid charge transfer kinetics enabled by the conductive nanofiber network allows for high power delivery, making PPy-based CNFs suitable for applications that require quick energy release. The increased capacitance and improved energy storage capability also contribute to higher energy densities, enabling prolonged operation and advanced energy storage capacity [90]. To further enhance the performance of PPy-based CNFs, various composite materials have been investigated and listed together with different PPy-based compounds in Table 1.

3.2. Polythiophene (PTh) fibers

PTh has arisen as a highly favorable material for SCs among various conducting polymers and has garnered significant attention [105–107]. It is an organic polymer synthesized through oxidative polymerization of thiophene monomers, possessing a highly conjugated structure with alternating single and double bonds that provide electrical conductivity. PTh is a versatile material that can be doped with various ions to enhance conductivity. In the investigation of Fu et al. [105], Electropolymerization of PTh films onto an MWCNT electrode was effectively achieved within an ionic liquid solution. The CV plots exhibit distinct polymerization behavior on MWCNT/glassy carbon (GC) and bare GC electrodes. The results from CV and GCD tests indicate that the PTh/MWCNT composites produced from the ionic liquid solution exhibit excellent capacitive properties that outperform those of MWCNT and pure PTh. The specific capacitance of the resulting SCs is 110 F g^{-1}. Additionally, the SCs demonstrate high stability as the specific capacitance can maintain 90 % of the initial capacitance after 1000 consecutive charge-discharge cycles. PTh's remarkable feature is its ability to

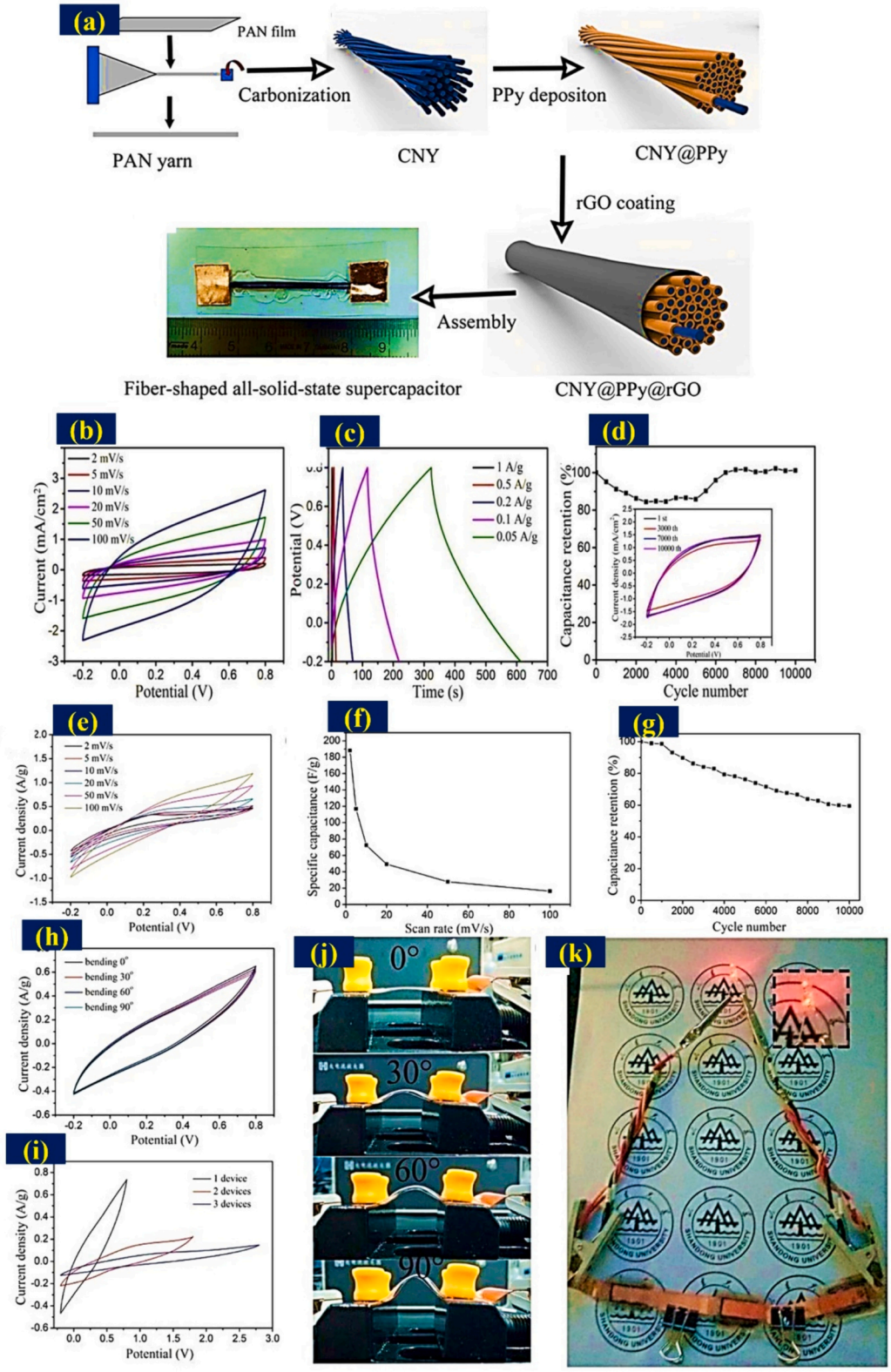

Fig. 3. (a) Step-by-step preparative process of CNY@RGO@PPy yarn-based flexible SCs through the carbonization of PAN film, PPy deposition, coating of RGO, and then assembling of two electrode cells (digital photograph demonstrates the fabricated flexible cell), reproduced with permission from Ref [85], (b–d) CNY electrode-based fiber structured solid-state SCs' electrochemical performance, including (b) CV profile at different sweep rates, (c) GCD at different current density rates, (d) long-term durability test at the sweep rate of 10 mV s^{-1}, reproduced with permission from Ref [85], (e) CV profile of as-made solid-state SCs at different sweep rates in the potential window of 1 V, (f) determined specific capacitance of as-made solid-state SCs at various sweep rates, (g) cyclic performance at 100 mV s^{-1} for as-constructed all solid-state SCs devices, (h) CV profile of ad-constructed solid-state SCs bent at various angles including 0–90° at 50 mV s^{-1}, (i) digital photographic images of solid-state SCs connected in series bent at various angles, and (j) optical photo image of LED powered using (k) three different solid-state SCs associated in series, reproduced with permission from Ref [86].

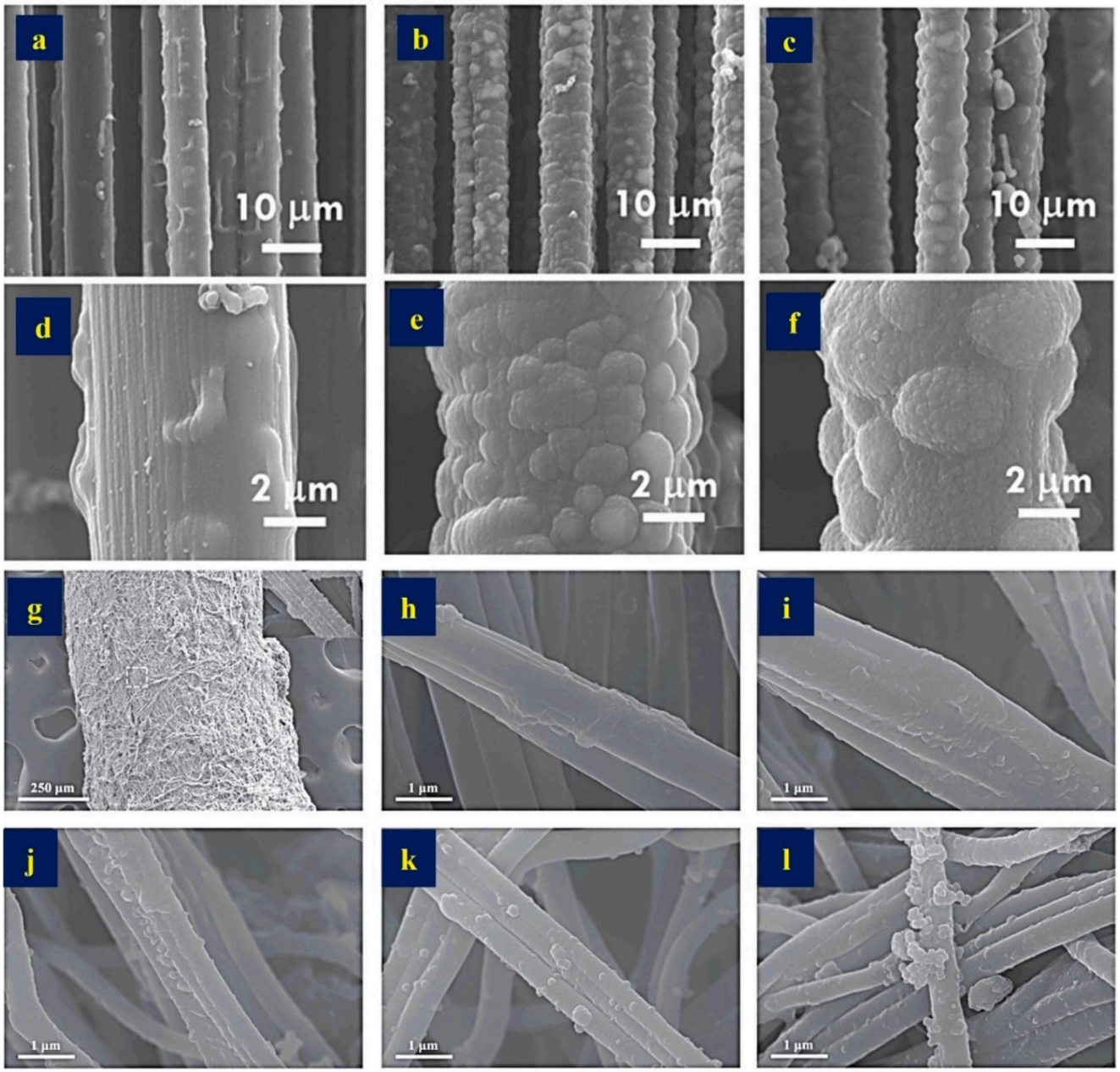

Fig. 4. (a–c) Low magnification FE-SEM micrographs of PPy@CNFs prepared by different electropolymerization applied potentials such as 10, 30, and 50 mV, (d–f) high magnification FE-SEM micrographs of PPy@CNFs prepared by different electropolymerization applied potentials such as 10, 30, and 50 mV, reproduced with permission from Ref [88], (g) FE-SEM images of pristine PAN@cotton yarn fiber, (h–l) different concentrations (0.1 to 0.5 M) of pyrrole monomer incorporated PAN@cotton yarn fiber, reproduced with permission from Ref [89].

alter its electrical conductivity in response to external stimuli such as temperature, pH, and light, making it a promising material for sensors and actuators. PTh-based CNFs possess a high specific SSA, which allows for enhanced electroactive sites and efficient charge storage. The porous structure of CNFs provides a large contact area for electrolyte ions, leading to improved ion adsorption and desorption kinetics. This increases capacitance, allowing the SCs to store more charge per unit mass or SSA. The inherent conductivity of PTh further facilitates the rapid transport of charge carriers, contributing to the overall capacitance enhancement [108,109]. The morphology and structure of PTh-based CNFs play a crucial role in enhancing the power density of SCs. The interconnected nanofiber network offers a high electrical conductivity pathway, minimizing the resistance during charge and discharge cycles. This enables efficient electron transfer and ion diffusion, leading to rapid charge transfer kinetics. As a result, PTh-based CNFs can deliver high power output, making them suitable for applications requiring quick energy delivery [110].

PTh-based CNFs contribute to the improved energy density in SCs through multiple mechanisms. Firstly, the unique morphology of CNFs provides a three-dimensional porous structure with a large SSA, allowing for a higher amount of charge to be stored. This increased SSA facilitates the adsorption and desorption of ions, leading to higher energy storage capacity. Additionally, using PTh as a precursor material ensures good electrical conductivity, which minimizes energy losses during charge/discharge cycles. As a result, PTh-based CNFs exhibit enhanced energy density, enabling the storage of a more significant amount of energy per unit mass [110,111]. For example, the controlled formation of PTh nanofibers anchored over TiO_2 nanotube array electrodes has

Table 1
The preparation techniques and electrochemical performance of several representative electrode materials for SCs based on PPy.

Device	ES condition	Specific surface area (SSA)	Carbonization temperature	Configuration	Morphology	Current density	Capacitance retention	Reference
$NiCo_2O_4$@PPy	10 kV		300 °C in air	Single electrode	Core-shell	4 A g^{-1}	90 % (5000 cycles)	[91]
PPy@LDH		122.5 m^2 g^{-1}	60 °C in vacuum	Single electrode	Core-shell	10 A g^{-1}	90.7 % (2000 cycles)	[82]
FEG/PPy-NS	19 kV, 1.9 ml h^{-1}		60 °C in vacuum	Single electrode	Composite	4 mA cm^{-2}	97.5 % (10,000 cycles)	[92]
SWCNTs@MnO_2/PPy	3 cm, 15 kV, 10 mL h^{-1}			Single electrode	Hierarchical	1 A g^{-1}	94.4 % (10,000 cycles)	[93]
PPy hydrogel	20–45 cm, 30–45 kV	36 m^2 g^{-1}		Single electrode	Gel and porous	2.8 A g^{-1}	93 % (2000 cycles)	[94]
MnO_2@PPy	15 cm, 18 kV	20–40 m^2 g^{-1}	1000 °C	Symmetric cell	Core-shell	1 A cm^{-3}	86.7 % (1000 cycles)	[95]
CNT-PPy-HQ			60 °C in vacuum	Symmetric cell	Composite	1 A g^{-1}	103 %	[96]
PPy-RGO	10 cm, 15 kV		45 °C in the oven	Symmetric cell	Composite	25.6 A g^{-1}	98 % (1000 cycles)	[97]
PPy	20–45 cm, 30–45 kV	36 m^2 g^{-1}		Symmetric cell	Interconnected chain	10 A g^{-1}	98 % (10,000 cycles)	[98]
WO_3-RGO//PPy-RGO				Asymmetric cell	Sandwich	8.3 mA cm^{-3}	99.4 % (2000 cycles)	[99]
PPy-NGP//MnO_2-NPG			80 °C	Asymmetric cell	Composite	100 mV s^{-1}	85 % (2000 cycles)	[100]
FEG/PPy-NS//FEG/MnO_2	5 cm, 20 kV	250 m^2 g^{-1}	60 °C in vacuum	Asymmetric cell	Layered sheet	6 A g^{-1}	97 % (10,000 cycles)	[92]
RGO/cMWCNT//CFP/PPy		910 m^2 g^{-1}	95 °C	Asymmetric cell	Composite	1 A g^{-1}	93 % (2000 cycles)	[101]
WO_3@V_2O_5/PPy	10 cm, 10 kV, 2 mL h^{-1}		500 °C in air	Micro-SCs cell	Core-shell	600 mA cm^{-3}	93 % (3000 cycles)	[102]
MnO_2@PPy	15 cm, 18 kV		1000 °C	Wearable SCs	Core-shell	80 mA cm^{-3}	92 % (4950 cycles)	[103]
Fe_3O_4@PPy	12 cm,12–14 kV,4 μL min^{-1}		700 °C in Ar	Wearable SCs	Core-shell	4.4 mA cm^{-2}	77 % (1000 cycles)	[104]

been designed by Ambade and his co-workers and employed for its potential applications in high-performance SCs [112]. The schematic illustration of the formation of PTh fiber over a TiO_2 nanotube array (PTh-TiO_2-NT/NF) is demonstrated in Fig. 5(a). The electrochemical behavior of the fabricated PTh-TiO_2-NT/NF electrode was evaluated through CV, GCD, and EIS analyses, as shown in Fig. 5(b–g). The CV profile suggests that the current density of PTh-TiO_2-NT/NF is more significant than that of the pristine TiO_2-NT/NF (Fig. 5(c)). The electrochemical performance of the PTh-TiO_2-NT/NF electrode is further evaluated by conducting the CV analysis at different scan rates, as shown in Fig. 5(d), which shows the increase in current density with scan rate implying the excellent pseudocapacitive nature of the PTh-TiO_2-NT/NF electrode. Further, the electrode exhibited a high capacitance of 1052 F g^{-1} (Fig. 5(d)) with excellent retention over 5000 cycles (Fig. 5(e)), indicating its electrochemical storage ability. The superb energy and power densities of 51.4 Wh kg^{-1} and 255.2 W kg^{-1} are the added beneficial properties of the PTh-TiO_2-NT/NF electrode. The symmetric behavior of the prepared electrode is further evaluated by conducting the GCD at different current density rates, as shown in Fig. 5(f), indicating the equivalent charge and discharge times. Their corresponding low R_{CT} value in the EIS analysis (Fig. 5(g)) confirms its excellent electrochemical characteristics. The fibers with an average diameter of 0.5 and 0.5 μm and smooth surface have been recorded for the prepared fibers through FE-SEM analysis. The authors concluded that PTh in the fiber structure improves connectivity and has electrochemical advantages for PAN fibers during the GCD process. Further, the conductivity of the fibers is strongly influenced by the concentration of PTh in the PAN's matrix.

A detailed investigation has been devoted to forming stretchable conducting PTh electrodes by depositing thiophene and 3-methyl thiophene over the stainless steel 304 (SS 304) by electro-polymerization by Wan and his team [74]. Further, using a serpentine wire, flexible SCs are fabricated (Fig. 5(h, i)) using these stretchable electrodes with PVA/H_2SO_4 gel electrolyte. The electro-polymerization of PTh, P3MTh is explained in brief as follows: As displayed in Fig. 5(j, k), the electropolymerization of PTh, P3MTh is conducted at a fixed scan rate of 100 mV s^{-1} in the potential windows of −0.2 to 1.25 and − 0.6 to 1.4 V respectively. Concerning the number of CV scans, the current density also increases, suggesting that the number of electrode materials over the SS 304 wire's surface is also enhanced. The resultant flexible SCs deliver the areal volumetric capacity of 87.2 μF cm^{-2} with an excellent capacity retention of 93 % over 10,000 cycles. Thakur and his team developed a similar PTh/MWCNT composite electrode through electropolymerization and achieved the excellent specific capacitance of 125 F g^{-1} at a low current density rate [113]. Very recently, electrospun PAN/PTh fibers have been developed by Maslakci et al. using the fixed concentration of PAN (10 %) and varied concentrations of PTh (1 and 3 %) through the ES process [114].

Various carbon materials have been investigated with different types of PTh-based compounds to improve the performance of PTh-based CNFs further. Azimi prepared PTh/GO nanocomposites through in situ polymerization and chemical reduction. The electrochemical characterization revealed that the PTh/GO nanocomposites exhibited remarkable capacitive properties. Specifically, at a scanning rate of 5.0 mV s^{-1}, the specific capacitance of the PTh/GO sample reached an impressive value of 28.68 F g^{-1}, surpassing the specific capacitance of the pure PTh material by a significant margin [115]. Rahman synthesized G nanoplatelets (GNPLs)/PTh composites with different mass ratios using an in situ oxidative polymerization method. Among the various samples prepared, the 50 % GNPLs/PTh composite demonstrated the highest specific capacitance, reaching 673.0 F g^{-1} at an operating current density of 0.25 A g^{-1}. Furthermore, this composite exhibited favorable cyclic stability, maintaining a capacity retention rate of 84.9 % after 1500 GCD cycles, with a scanning rate of 50 mV s^{-1} [116]. So far, the studies on PTh/metal oxide composite electrode materials for SCs are minimal because of the relatively lower electrochemical performance of PTh compared to PANI and PPy [117].

Regarding the morphological and particle size aspects of PTh and its

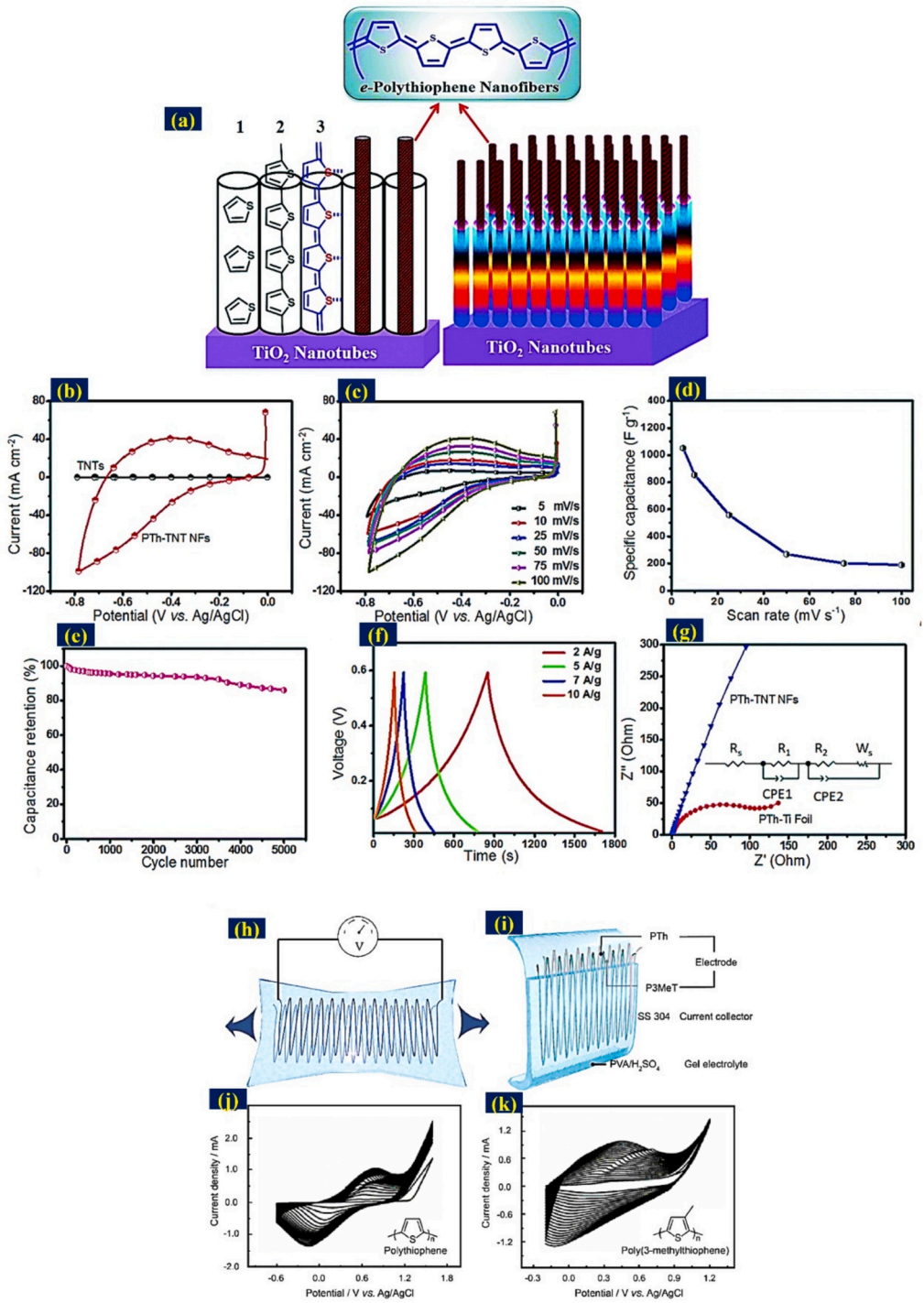

Fig. 5. (a) Graphical illustration of one-dimensional PTh-nanofibers grown over the 1D TiO_2 nanotubes through electropolymerization process, (b–g) electrochemical properties of PTh-TiO_2 NTs prepared through electropolymerization of Th monomer (0.5 M): (b) CV profile of pristine TiO_2 NTs and PTh-nanofibers at the constant scan rate of 100 mV s^{-1}, (c) CV profile of PTh-TiO_2 NTs at various scan rates (5–100 mV s^{-1}) in the potential window between −0.8 and 0 V, (d) calculated specific capacitance values of PTh-TiO_2 NTs at various scan rates, (e) its corresponding long term durability test over 5000 GCD cycles, (f) GCD profile of PTh-TiO_2 NTs at various current density rates ranging from 2 to 10 A g^{-1}, (g) its respective impedance Nyquist plot with equivalent circuit, reproduced with permission from Ref [112], (h, i) design and schematic illustration of the flexible SCs using gel polymer electrolyte and P3Me-Th-based electrode, (j, k) continuous CV profile PTh and P3Me-Th electrodes in 0.2 M electrolyte-buffer solution, reproduced with permission from Ref [74].

composite-derived CNFs, it is essential to note that the morphology and particle size distribution significantly impact the electrochemical performance of SCs. The morphology of PTh-based CNFs can be controlled through various synthesis methods, such as ES, template-assisted synthesis, or chemical vapor deposition, which can tailor the morphology of the CNFs to optimize their performance. For instance, controlling the diameter and length of the nanofibers allows for increased SSA and improved electrolyte accessibility, which directly influences the SCs' capacitance and energy storage capabilities [111]. Similarly, the particle size distribution of PTh-based CNFs affects the electrochemical behavior of the SCs. Uniform and well-defined particle sizes ensure uniform charge distribution and effective ion transport within the nanofiber

network, improving performance. On the other hand, a broad particle size distribution may result in uneven charge storage and hinder efficient ion diffusion, consequently impacting the capacitance and power density [90]. For instance, Matysiak et al. have produced a sequence of composite CNFs using the ES process from PAN/DMF solutions with various CPs, including PANI, PPy, and PTh [118]. The pristine PTh nanopowder has an average particle diameter of 131 nm, which is inferred through SEM and particle size distribution analyses, as shown in Fig. 6(a, b). The smallest diameter of separate particles of PTh with different concentrations (1 % and 3 %) was incorporated into PAN/DMF solutions, which did not produce any defects in the resultant composite, as shown in Fig. 6(c, e). The average particle diameter of these composites is much smaller than the pristine PAN samples, and it was in the range of 200 to 650 nm (Fig. 6(d, f)). These composites would be suitable for ideal energy storage and conversion applications. Later, Momin and his team reported a series of nanocomposite fibers comprising PTh, MWCNT, and Ru/Pd nanoparticles for improved storage performance [119]. The FE-SEM micrographs of PTh, PTh/MWCNT, PTh/MWCNT/Ru/Pd are displayed in Fig. 6(g–i). These layer stacking PTh/MWCNT/Ru/Pd composite showed a thick PTh was wrapped and decorated over the MWCNT, which enhances the overall conductivity of MWCNT by the layer-by-layer stacking. Owing to these specific morphologies, the reported electrode showed outstanding capacitance, specific energy, and power of 86 F g^{-1}, 10.7 Wh kg^{-1}, and 280.4 W kg^{-1}, respectively.

3.3. Polyaniline (PANI) fibers

Plenty of conducting polymers such as PANI, PPy, PTh, and poly (3,4-ethylene dioxythiophene) (PEDOT) have been explored for the construction of 1D nano-architecture so far [117,120]. Between them, PANI is an important and pioneered conducting polymer for its excellent intrinsic electrical conductivity. It has vast, interesting properties due to its high stability, simple fabrication process, feasibility to alter the oxidation state, good electrical conductivity, etc. PANI could be either electrically conductive or insulator based on its electronic oxidation states. It exhibits valence states, including pernigraniline, emeraldine, and leucoemeraldine [46].PANI can be synthesized through both chemical and electrochemical routes by oxidative polymerization of aniline monomers [121]. Following Conway's seminal paper, PANI has arisen as one of the favorable candidates for SCs [122]. A new electrospun polyethylene oxide (PEO)-PANI fiber has been synthesized using secondary dopant cresol and reported by Bhattacharya et al. [123]. Using various ES solvents such as chloroform, chloroform-dimethyl formamide (DMF), and various ratios of chloroform and cresol such as (9:1 and 4:1), they have developed four different fibers as shown in Fig. 7(a). It is evident from the figure that the inclusion of m-cresol leads to the chain extension of PANI fibers, resulting in improved conductivity than DMF solvent-based fibers. The 4:1 chloroform-cresol-based PANI-PEO fiber has shown the highest conductivity of 1.73 S cm^{-1} under ambient conditions. The ultra-high specific capacitance of 3121 F g^{-1} at

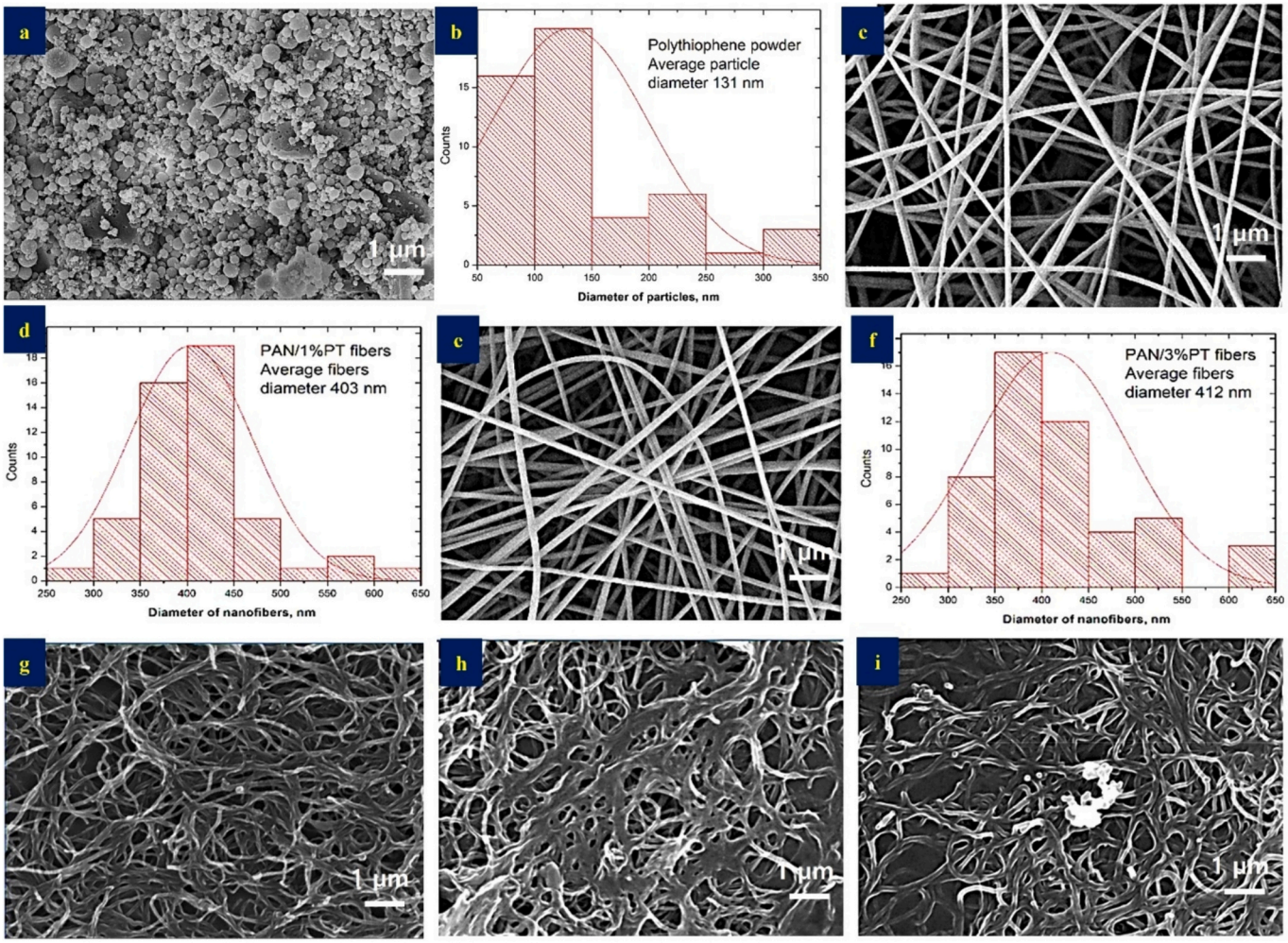

Fig. 6. (a, b) SEM image and particle size distribution results of pristine PTh nanopowder, (d–f) FE-SEM and particle size distribution results of 1 % and 3 % PTh incorporated PAN fibers, reproduced with permission from Ref [118], (g–i) FE-SEM images of pristine PTh, PTh/MWCNT, and PTh/MWCNT/Ru/Pd composites, reproduced with permission from Ref [119].

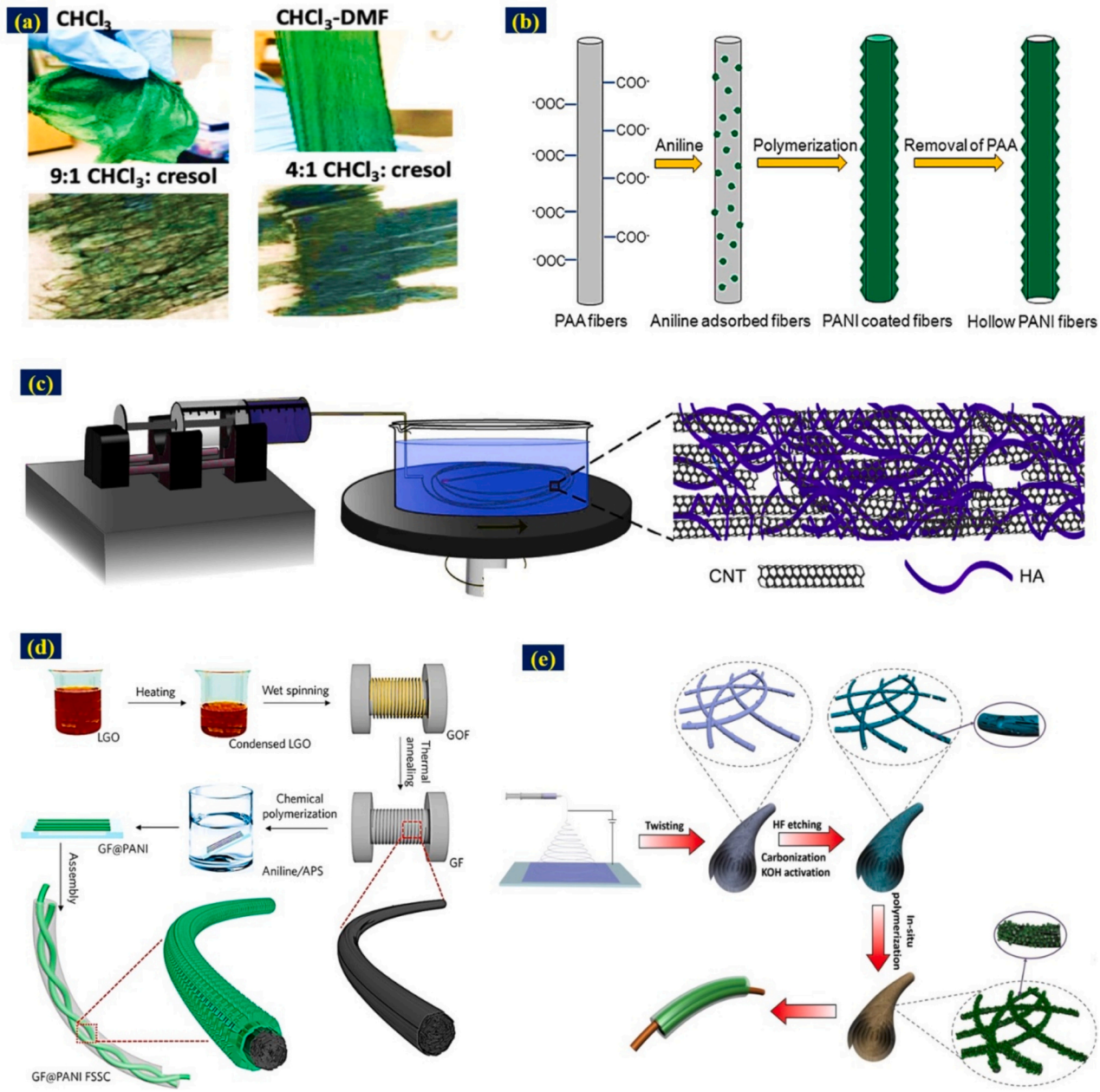

Fig. 7. (a) Solubility behavior of PANI-PEO blend electrode in various concentrations of chloroform: cresol solvent mixture, bottom images represent their corresponding spun-fibers in different solvents, reproduced with the permission from Ref [123], (b) typical illustration for the formation process of hollow PANI NFs, reproduced with permission from Ref [125], (c) schematical illustration of the construction of HA-CNFs using the wet-spinning method, reproduced with permission from Ref [130], (d) graphical sketch for the formation of PANI@GE foam, fabricated two electrode flexible SCs device and structure of PANI@GE foam, reproduced with the permission from Ref [131], and (e) a typical representation of the preparative methods of PANI-NCNFs, reproduced with permission from Ref [133].

0.1 A g^{-1} was recorded for the same electrode. Wang and co-workers developed PANI nanofibers as plausible electrode materials for high-energy SCs [124]. The stepwise fabrication of hollow PANI fibers from PAA is demonstrated in Fig. 7(b) [125]. Before in-situ polymerization of aniline, the electrospun PAA was fabricated using the following ES conditions of 18–25 kV applied voltage, 0.5 mm spinneret syringe diameter, 0.25 mL h^{-1} flow rate, etc. Under 1 M H_2SO_4 medium, the proposed hollow PANI fiber electrode has delivered the maximum capacitance of 605 F $g^{-1,}$ which might be attributed to ordered pore passages, thin wall thickness, and hollow morphological features. Subsequently, Rudge and his colleagues have investigated the doping effect of PANI on its supercapacitive properties and demonstrated that it exhibits superior performance over its battery counterparts [126,127]. Nanocomposites incorporating PANI and carbon nanomaterials, such as CNTs, RGO, and G, are commonly employed in SCs fabrication. Among the first high SSA carbon nanomaterials, CNTs, either in SWCNT or MWCNT form and G, have been effectively utilized to enhance the electrochemical performance of PANI-based SCs [128]. In this regard, an electrospun fibrous electrode comprised of PANI/MWCNT has been constructed by Liang and co-workers [129]. By changing the ES experimental conditions, such as needle-to-collector distance (8 to 14 cm), ES voltage (6.1 to 9 kV), and flow rate (1 to 3.5 μL min^{-1}), the microstructure of the PANI/MWCNT electrode could be tuned. For instance, when the needle-to-collector distance has changed from 80 to 140 mm, the SSA of the electrode has improved from 57 to 83 m^2 $g^{-1,}$ and the average diameter of the fiber decreases from 2.89 to 1.21 μm. During these changes in ES conditions, using PVA/H_2SO_4 electrolyte, the electrochemical capacitance has also improved from 130 to 180 F g^{-1}. From

their observations, it has been concluded that the change in the ES parameter for the electrode formation has a substantial role in examining the physicochemical and electrochemical properties of the SCs.

Later, a PANI-anchored hyaluronic acid (HA)-CNT microfiber was fabricated by combining the wet-spinning process and electrochemical polymerization techniques, as demonstrated in Fig. 7(c) [130]. Fig. 7(c) shows that this process involves the flow rate and high power sonic of 50 mL h^{-1} and 500 W, respectively. The resultant PANI-HA-CNT microfiber offers a sixfold increase in capacitance with an excellent retention percentage of 90 % even after 3000 cycles. Moreover, the consequent PANI-HA-CNT microfibers are highly conductive and possess high mechanical stability. Similarly, using GE fibers, a PANI-GE fiber composite electrode has been designed and developed by combined wet-spinning and thermal annealing processes and reported as a potential candidate for flexible SCs [131]. The typical fabrication process for the formation of composite PANI-GE fiber is sketched in Fig. 7 (d). Under 1 M H_2SO_4 electrolyte medium, the resultant electrode has delivered excellent electrochemical performance with the capacitance, energy density, and power density of 357.1 mF cm^{-2}, 7.93 μWh cm^{-2}, and 0.23 mW cm^{-2} respectively. In addition, it has displayed an outstanding retention property with 78.9 % even after 5000 GCD cycles, confirming its excellent rate capability. When a bare PANI is incorporated into CNFs, it further enhances the overall performance of SCs, leading to improved capacitance, power density, and energy density. The presence of PANI in CNFs significantly enhances the capacitance of the electrode material. PANI offers pseudocapacitance, which arises from the reversible redox reactions at its surface. This additional capacitance contributes to the overall charge storage capability of the SCs, enabling higher energy storage. The redox reactions of PANI result in Faradaic charge transfer, which complements the non-faradaic charge storage mechanism of the CNFs, resulting in enhanced overall capacitance [128,132]. For instance, Yang and his team have assembled fiber-shaped SCs using PANI nanopillars anchored over 3D hierarchical N-doped CNFs [133]. The preparation process of N-doped CNF involves the ES process of PAN-SiO_2, stabilization of PAN-SiO_2 at 280 °C for 2 h, KOH activation, and followed by HF etching for 12 h to remove SiO_2 to produce the N-doped CNFs. Later, oxidative polymerization of aniline in N-doped CNF in the presence of HCl and ammonium persulfate solution yields the final PANI nanopillar-NCNF composite electrode, as demonstrated in Fig. 7(e). They have also constructed bare NCNF for comparison purposes. Compared to the bare electrode, the composite electrode achieves the highest capacitance of 339.3 F g^{-1} with an excellent energy density of 11.6 Wh kg^{-1}. The improved electrochemical performance might be attributed to the synergism between the PANI nanopillar array and the 3D interconnected NCNFs' porous structures.

PANI and its composite-derived CNFs offer unique morphological and particle size advantages. Depending on the synthesis method and conditions, PANI can exhibit various morphologies, such as nanofibers, nanotubes, or nanoparticles. These morphological variations affect the SSA, porosity, and accessibility of the active material, influencing electrochemical performance. For instance, PANI nanofibers provide a higher SSA and better electrode-electrolyte contact, promoting efficient charge transfer and enhanced capacitance. In the case of composite-derived CNFs, the morphology and particle size of PANI plays a

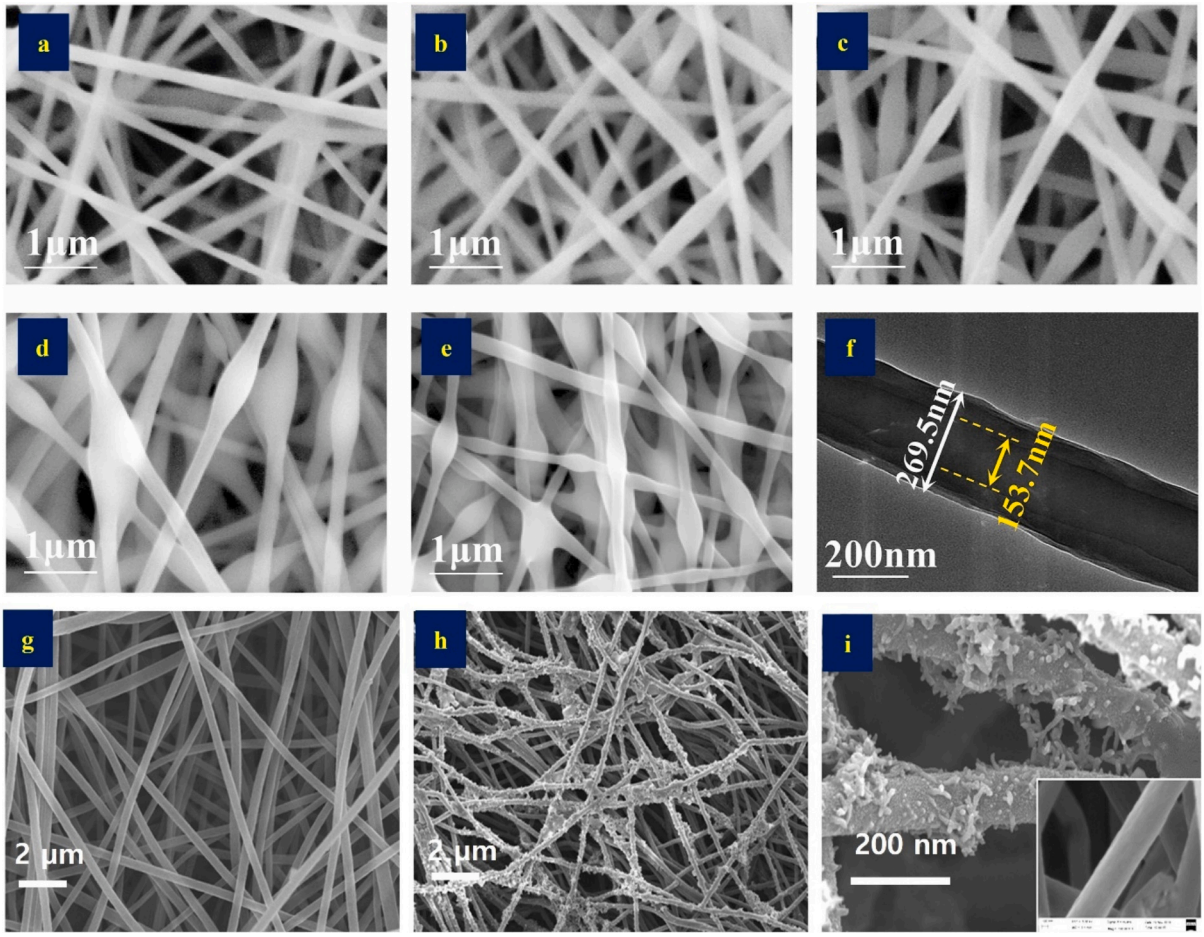

Fig. 8. (a) FE-SEM micrographs of PEI@PANI CFM fibers with various core/shell flow rate ratios ranging from 1 to 5, (f) its corresponding HR-TEM image indicates lighter PANI shell with the thickness of 269.5 nm and dark core of PEI with the diameter of 153.7 nm, reproduced with the permission from Ref [134], (g–i) FE-SEM images of PANI fiber and different concentrations of CNFs mats incorporated PANI/CNFs mats, reproduced with permission from Ref [135].

crucial role. The dispersion of PANI within the CNFs' matrix affects the accessibility of active sites and the overall electrode performance. Proper distribution and integration of PANI particles within CNFs enhance the synergistic effects, ensuring effective utilization of PANI's capacitance and improving the overall electrochemical performance of SCs. Wang and his colleagues have developed innovative polyetherimide@PANI core-shell fibrous membranes (PEI@PANI CFMs) through a coaxial ES process [134]. Using PEI, emeraldine base PANI (EB-PANI) with high concentration could be precisely decorated over the fiber's surface, affirming the high hydrophilicity, excellent pore structures, good mechanical stability, and outstanding electrical conductivity. Fig. 8(a–e) shows the FE-SEM results of PEI@PANI CFMs with various core-shell flow rate ratios. The micrograph shows that the electrospun PEI@PANI CFMs comprise a 3D network containing different fiber orientations and show a polyporous structure. In that polyporous morphology, the submicron particles are interconnected with one another. No beads were formed at a low flow rate, and uniform fibers were obtained (Fig. 8(a–c)), whereas, at a high flow rate, the interconnected nodes with uneven fibers were formed (Fig. 8(d, e)). Fig. 8(f) shows that its corresponding TEM showed a visible boundary between the core and shell with the PANI light shell and dark PEI core with an average diameter of 270 nm and 153 nm, respectively. These morphological results indicate the successful formation of PEI@PANI CFM. Owing to this specific architecture, the resultant electrode showed outstanding areal capacitance and energy density of 1159 mF cm^{-2} and 46.9 μW h cm^{-2}, suggesting excellent capability for flexible SCs.

Surabhi and her team explored the simple fabrication process to prepare free-standing PANI/CNFs-based hybrid mats for improved storage performance obtained from the EDLC of CNFs and PC of PANI [135]. The microstructure of the prepared hybrid mats was evaluated by FE-SEM analysis, which showed a distinct microstructure between the pristine CNFs and PANi/CNFs mat. A smooth, uniform surface was observed for the pristine sample, whereas the more undulated rough surfaces were observed for the hybrid mats (Fig. 8(g, h)). Further, the diameter of the core-shell PANI is relatively larger than the pristine CNFs (Fig. 8(i)). The proposed electrode mats delivered the highest gravimetric capacitance of 493.7 F g^{-1} at 1 mA cm^{-2}. The energy and power densities were nearly 68.6 Wh kg^{-1} and 8300 W kg^{-1}. These studies pave the way to move a step forward to prepare flexible, cost-effective, high-energy SCs.

Moreover, incorporating PANI into CNFs improves the energy and power density of the SCs. The high conductivity of PANI facilitates rapid electron transfer, enabling efficient charge/discharge processes. This leads to a reduction in the internal resistance and improved power delivery of the SCs. The combination of PANI's conductivity and the high SSA of CNFs allows for faster ion transport and reduced diffusion

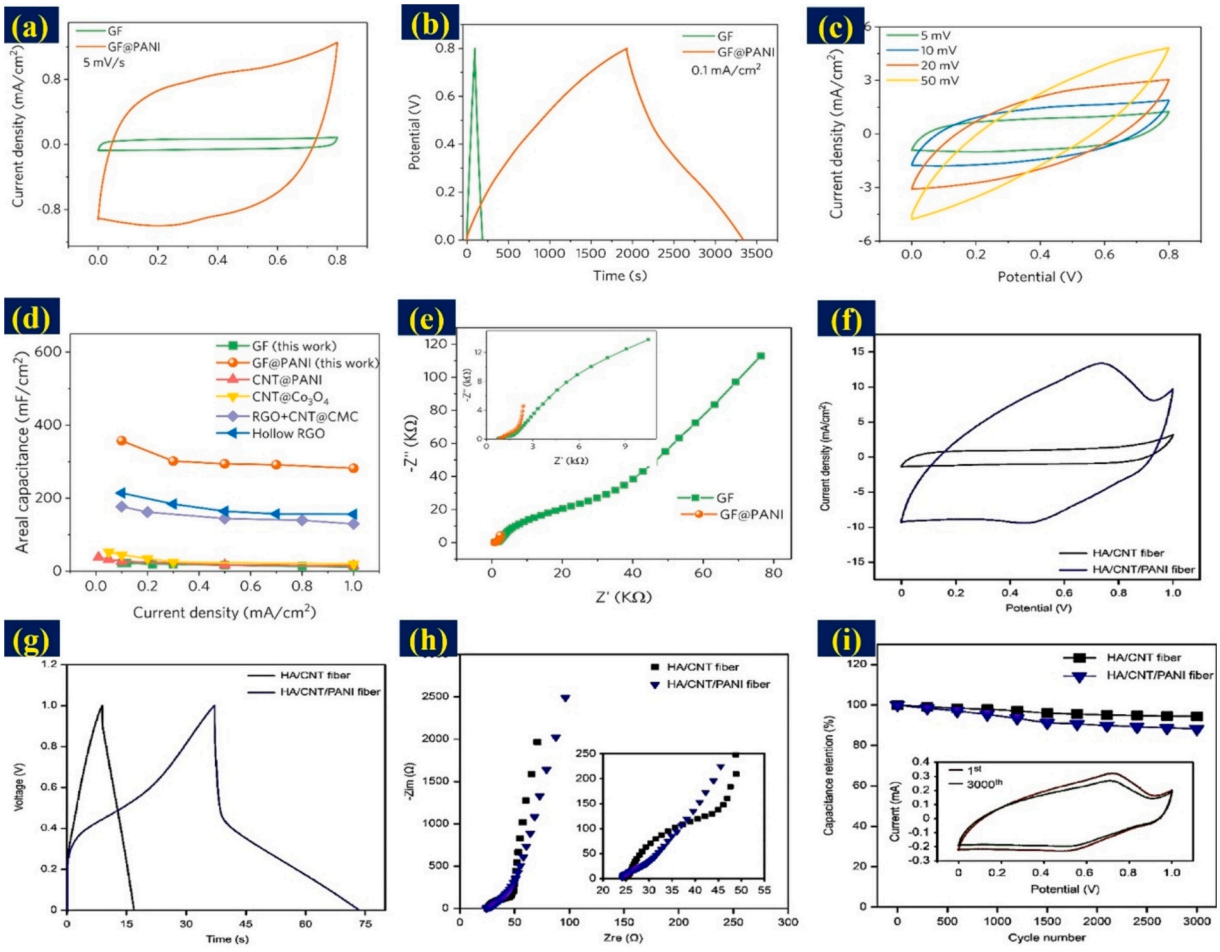

Fig. 9. (a) CV profile comparison of GE foam and GE foam@PANI electrodes at the fixed scan rate of 5 mV s^{-1}, (b) GCD comparison plot of GE foam and GE foam@PANI electrodes at the fixed scan rate of 0.1 mA cm^{-2}, (c) CV profile of GE foam@PANI at various scan rates ranging from 5 to 50 mV s^{-1} in the potential range of 0 to 0.8 V, (d) areal capacitance as a function of current density for GE foam@PANI with various reported carbon electrodes, (e) comparison Nyquist plots of pristine GE foam and GE foam@PANI electrodes based flexible SCs, reproduced with the permission from Ref [131]; (f) CV profile comparison of HA/CNT and HA/CNT@PANI electrodes, (g) GCD profile of HA/CNT@PANI at different current density rates, (h) Nyquist impedance diagram of bare HA/CNT and HA/CNT@PANI electrodes, and (i) long term durability test over 3000 cycles, inset CV profile demonstrates the first and 3000 CV cycles, reproduced with the permission from Ref [130].

limitations, resulting in higher power density [136]. PANI's redox properties and high capacitance enable the storage of a more significant amount of charge per unit mass or volume. Combining PANI's pseudo-capacitance and the double-layer capacitance of CNFs leads to a synergistic effect, enhancing energy storage capabilities. This translates into higher energy density, allowing SCs to store more energy for a given size or weight. Some classical examples are explained herein. As demonstrated earlier, when PANI is introduced into GE fiber, it drastically improves the electrochemical properties of the resultant material [131], as shown in Fig. 9(a–e). As demonstrated in Fig. 9(a, b), the integral area of the CV curve (with the potential window of 0.8 V) and discharge time for the PANI-GE fiber composite have improved 12-fold more than its pristine counterpart. Further, the electrochemical stability is proved by the increase in current density and discharge time concerning sweep, as demonstrated in Fig. 9(c). The as-prepared PANI-GE fiber composite delivers the highest capacitance of 314.5 mF cm^{-2}, twelve times greater than bare GE foam, as shown in Fig. 9(d). The low R_T value of the composite, as shown in Fig. 9(e), implies its excellent electrochemical transport behavior. Similarly, the PANI-HA-CNT microfiber is another classic example of the improved electrochemical properties of carbon-based material after the addition of PANI [130]. Its corresponding electrochemical and cycling stability properties are shown in Fig. 9(f–i). The increment in the integral area of the CV plot (Fig. 9(f)) improved discharge time in GCD (Fig. 9(g)), confirming the composite is much better than the bare electrode. Fig. 9(h) shows that the composite's R_{CT} and R_s values are much lower than pristine, indicating excellent charge transport behavior. In addition, the composite electrode possessed a much-improved retention percentage over 3000 GCD cycles than the pristine one (Fig. 9(i)), which might be mainly due to the synergistic effect between the PANI, HA, and CNT microfibers. Very recently, an interesting approach was found, including simultaneous ES and electrospraying processes for fabricating a PANI-carbon nanoparticle hybrid for the enhanced performance of hybrid SCs, by Chen et al. [137]. The electrode affords a high capacitance of 235 F g^{-1} at 1 A g^{-1} with a capacitance retention of 67 % over 1000 GCD cycles.

A selective surface diffusion processed PANI-C-AC (polyaniline cellulose derived porous activated carbon) electrode has been prepared by Zhang and the team through the two-step ES cum selective surface diffusion process [138]. The PANI nanorods have uniformly grown over the porous 3D fibers. The ES process for preparing the fibers was performed under the following conditions: a flow rate of 1.2 mL h^{-1} and an applied potential of 5–7 kV. The resultant electrode possesses the highest surface area of 2402 m^2 g^{-1} with outstanding electrochemical properties, such as capacitance of 765 F g^{-1} and 91 % retention even after 5000 GCD cycles. On the other hand, the ES-processed PANI/hollow CNFs provide a hollow nanofiber with an enhanced surface area 2.03 times greater than that of the pristine fiber [139]. The calcination temperature was maintained at 1300 °C for 3 h for preparation. It yields a maximum capacitance of 1196 F g^{-1} at 1 A g^{-1} with a capacitance retention of 90 % over 3000 cycles. In the meantime, Ataram et al. have prepared a ternary composite comprised of PANI@$NiFe_2S_4$@CNFs through the combination of ES (flow rate-0.8 μL min^{-1}, voltage-20 kV, distance-15 cm) and calcination processes (600 °C for 1 h) [140]. The as-prepared electrode was reported to have the highest capacitance of 645

Table 2
Some typical PANI and PEDOT-based SCs electrode materials' preparation methods and electrochemical performance.

Materials	ES condition	Specific surface area (SSA)	Carbonization temperature	Morphology	Preparation method	Maximum specific capacitance	Cycle stability	Ref.
PANI/C-ACs	5–7 kV, 0.3–1.25 ml h^{-1}	2402 m^2 g^{-1}	150 °C in vacuum	3D porous	Selective surface dissolution (SSD) method	765 F g^{-1} at 1 A g^{-1}	91 % after 5000 cycles	[138]
PANI/PEO fibers	1.5 μL min^{-1}, 25 kV, 20–26 cm	–	–	Fiber mat	ES process	3121 F g^{-1} at 0.1 A g^{-1}	85 % after 80 cycles	[123]
PANI @hollow CNFs	0.8 μL min^{-1}, 12 kV, 20–18 cm	2.03 times >CNFs	1300 °C for 3 h	Hollow nanofibers	ES process	1196 F g^{-1} at 1 A g^{-1}	90.1 % after 3000 cycles	[139]
CNFs@$NiFe_2S_4$@PANI	0.8 μL min^{-1}, 20 kV, 15 cm	–	600 °C for 1 h	Nanoparticles anchored fibers	ES process	645 F g^{-1} at 1 A g^{-1}	78 % after 5000 cycles	[140]
N-doped PAN/PANI CNFs	0.5 μL min^{-1}, 15 kV, 15 cm	534.1 m^2 g^{-1}	800 & 900 °C	Porous fibers	ES process	199.5 F g^{-1} @ 1 A g^{-1}	82 % after 1000 cycles	[141]
EB-PANI	–	44 m^2 g^{-1}	220 °C	Porous	Dissolution of hydrochloride and ammonium persulfate	260(±5) F g^{-1} at 3 mV s^{-1}	–	[154]
GE foam@PANI	–	34.8 m^2 g^{-1}	800 °C	mesoporous	GE foam wet spinning, doped with aniline	66.6 mF cm^{-2}	–	[155]
PANI-HCNFs	12 cm, 15 kV, 1 mL h^{-1}	734 m^2 g^{-1}	900 °C under Ar/H_2	Interconnected, porous	Aniline, HCNFs oxidation	339.3 F g^{-1} at 0.5 A g^{-1}	74.2 % after 3000 cycles	[90]
P-f-CNFs/PEDOT/MnO_2	–	281 m^2 g^{-1}	–	Porous	–	776.7 F g^{-1} at 25 mV s^{-1}	104.6 % after 5000 cycles	[156]
PEDOT@N-doped CNFs	150 W, 1.5 h, 15 kV, 19 cm	107 m^2 g^{-1}	800 °C (2 h)	Fibers with typical layer-like structure	Vapor oxidative polymerization	203 F g^{-1}	87 % after 10,000 cycles	[146]
PEDOT:PSS NFs	1.5 μL min^{-1}, 18 kV, 15 cm	–	150 °C (30 min)	Porous fibers	–	1.8 mF cm^{-2} at 5 μA cm^{-2}	90 % after 10,000 cycles	[150]
PEDOT:PSS NFs	2 mL h^{-1}; 8 s/r	–	–	Nanofibers	Wet-spinning	188.5 F cm^{-3}	80 % after 1.9 million cycles	[152]
PEDOT/Nafion	–	–	Room temperature	Rough, thin film	Sonication process	74 F cm^{-3}	98.7 % after 1000 cycles	[153]
PEDOT:SSEBS NFs	5 mL h^{-1}; 18 kV; 15 cm	–	60 °C for 3 h	Microfiber mat	Coaxial ES process	990 mF cm^{-2} at 1 mA cm^{-2}	99 % after 5000 cycles	[149]

PANI-poly aniline; EB-emeraldine; GE-graphene; PEDOT:PSS-poly(3,4-ethylenedioxythiophene)–poly(styrenesulfonate); SSEBS: polystyrene-*block*-poly(ethylene-*ran*-butylene)-*block*-polystyrene; NFs-nanofibers; CNFs-carbon nanofibers; ES-electrospinning

F g^{-1} and a moderate retention of 78 % (5000 cycles). Later, lignin-derived N-doped PAN CNFs that combined with PANI (N-doped PAN/PANI CNFs) electrodes were prepared by ES (flow rate-0.5 μL min^{-1}, voltage-15 kV, distance-15 cm) and calcination processes (800 & 900 °C) [141]. These porous fiber electrodes provide the superior capacitance of 199.5 F g^{-1} at 1 A g^{-1} with excellent capacitance retention over 10,000 GCD cycles (82 %).

Table 2 implies various electrospun PANI-based composite materials' structural and electrochemical parameters for improved SCs' performance.

Using bare PANI-based CNFs in SCs improves capacitance, power, and energy density. The unique properties of PANI, along with the advantageous morphological and particle size aspects, contribute to the enhanced electrochemical performance of the composite material. This paves the way for developing high-performance SCs with increased energy storage capabilities for various applications.

3.4. Poly(3,4-ethylene dioxythiophene) (PEDOT) fibers

PEDOT is a remarkable conducting polymer that has revolutionized the field of organic electronics. PEDOT has garnered significant attention as an extensively studied and widely employed material due to its exceptional electrical conductivity, unique chemical and physical properties, swift electrochemical kinetics, and outstanding intrinsic conductivity, surpassing other conducting polymers [142,143]. The synthesis of PEDOT involves the polymerization of 3,4-ethylenedioxythiophene monomers, typically using oxidative chemical or electrochemical methods. The polymerization process produces a highly conjugated structure, where the thiophene rings form an extended π-conjugated backbone. This delocalized π-electron system is responsible for the impressive electrical conductivity observed in PEDOT, enabling efficient charge transport.

One of the notable features of PEDOT is its inherent stability in air and moisture, which sets it apart from many other conducting polymers. This stability arises from the methylenedioxy groups attached to the thiophene rings, which act as protective barriers, preventing unwanted oxidation and degradation. The robustness of PEDOT makes it a suitable material for applications requiring long-term stability, such as flexible electronics and wearable devices. PEDOT exhibits exceptional processability, allowing its facile integration into various device architectures. It can be solution-processed, spin-coated, or deposited through vapor-phase techniques onto various substrates, including flexible and stretchable materials. This versatility in processing techniques makes PEDOT compatible with large-scale manufacturing processes, making it an attractive choice for commercial applications. Beyond its remarkable electrical conductivity, stability, and processability, PEDOT possesses additional desirable properties that further contribute to its appeal. For instance, PEDOT is transparent in its pristine state, enabling its use in transparent electrodes for applications like touchscreens and displays. Moreover, PEDOT is inherently flexible and mechanically robust, making it suitable for flexible electronics, where traditional brittle materials would fail. The broad range of applications for PEDOT is a testament to its unique properties and versatility. PEDOT is commonly used as a hole transport layer in organic solar cells, effectively transporting positive charges from light absorption to the electrode. OLEDs serve as a transparent electrode or a hole injection layer, facilitating the efficient flow of electrical current and enhancing device performance. PEDOT can also be employed in electrochromic devices, where its reversible color change upon oxidation or reduction enables applications in bright windows, displays, and electrochromic mirrors [71].

In the early 2010s, all textile SCs with excellent flexibility were first introduced by Laforgue et al. using PEDOT nanofibers [148]. The ES process assisted PEDOT nanofibers with an average diameter of 350 nm and excellent conductivity of 60 ± 10 S cm^{-1}. This improved conducting might be attributed to the ultra-porous nature of the PEDOT mats. While using PVdF-co-HFP-Ionic liquid gel electrolyte, the symmetric device achieved the highest capacitance of 85 F g^{-1}. By employing EDOT and SEBS monomers, highly flexible and stretchable PEDOT: SSEBS electrodes have been constructed by ES process (conditions: flow rate-1.5 μL min^{-1}, ES voltage-18 kV, distance-15 cm) at 60 °C for 3 h by Kolathodi and his team [149]. The proposed electrode shows a microfibrous mat morphology with 100 % capacitance retention and excellent capacitance of 1296 mF cm^{-2}. A highly conductive, flexible RGO/PEDOT: PSS/PVA composite fiber has been designed and developed by Yin et al. through the ES process [144], as shown in Fig. 10(a). The resultant composite fiber electrode possesses excellent ductility, better filterability, and high energy density. Further, the composite fiber has outstanding mechanical and electrical characteristics with a tensile stress of 4.7 MPa, radial elongation at break of 61.13 %, and electrical conductivity of 1.7 S cm^{-1}, which paves it to utilize as a promising candidate in high energy EES devices. Martinez and his fellow workers have recently constructed PEDOT: PSS nanofiber electrodes with excellent transparency and high flexibility through the ES process [150]. For the ES process, ethylene glycol was used as the potential solvent, and PET substrate was utilized as the substrate. The flexible, solid-state SCs yield the gravimetric and areal capacitances of 3.6 F g^{-1} and 1.8 mF cm^{-2}, respectively, stability over 1000 cycles with a retention percentage of 92 %, suggesting its practical viability.

Meanwhile, Abdah and his coworkers have synthesized porous functionalized PEDOT/MnO_2 fibers through combined ES and electropolymerization methods [145]. Using PAN: PTFE (polytetrafluoroethylene) polymers in the volume ratio of 2:3, an electrospun PAN: PTFE fiber was prepared initially. The designed fiber is then subjected to stabilization and functionalization processes to obtain the porous functionalized CNFs. The resultant CNFs undergo electro-polymerization with EDOT, followed by electrodeposition with MnO_2, producing the p-f-CNFs/PEDOT/MnO_2 composite, as shown in Fig. 10(b). On the other hand, highly conductive PEDOT fibers are produced through vapor-phase polymerization that begins with the electrochemical deposition of uniformly distributed Fe_2O_3 nanosheets on N-doped CNFs, as reported by Zhu and his team [146]. The surface morphology can be tuned by changing PEDOT's vapor polymerization time and mass loading. For instance, when the time is low, the FE-SEM results show particles along with the fiber, whereas, at high vapor polymerization time, they show only fibers, as shown in Fig. 10(c–e). These types of PEDOT-based CNFs show interesting electrochemical properties. For instance, the p-f-CNFs/PEDOT/MnO_2 composite discussed above exhibits an outstanding capacitance of 776 F g^{-1} in 1 M KCl at 25 mV s^{-1} [145]. The constructed asymmetric device gives the potential window of 1.6 V with the specific capacitance, energy density, and capacitance retention of 1061 F g^{-1}, 60.5 Wh kg^{-1}, and 104.5 %, respectively. These promising results suggest that the p-f-CNFs/PEDOT/MnO_2 composite could be a good candidate for next-generation SCs. The same research group later prepared a similar electrospun CNFs/PEDOT/MnO_2 composite electrode and utilized it as the positive electrode in high-performance SCs [151]. When tested with an AC negative electrode, the asymmetric device offers the highest potential window of 1.6 V and a specific capacitance of 537 F g^{-1} at 5 mV s^{-1}. Even after 8000 GCD cycles, the cell maintains 81.06 % of its initial capacitance, confirming its excellent durability. Further, they have investigated the effect of electrodeposited PEDOT over electrospun PVA-GO nanofiber and employed it as the potential SCs cathode electrode [147]. As demonstrated in Fig. 10(f), the CV plot of the fabricated cell shows a rectangular fashion with an increase in current density upon various scan rates. Fig. 10(g) shows that the compartment offers a capacitance as high as 224.5 F g^{-1} at 5 mV s^{-1}. The decrease in capacitance concerning sweep rates might be due to the less time the ions occupy over the PEDOT-GO surface. Further, it has produced a high voltage window of 1.8 V, suggesting their high electrochemical stability (Fig. 10(h)). These observations confirm that the proposed electrode could be suitable for future flexible electronics. Meanwhile, the wet ES process for preparing PEDOT: PSS NFs was performed under the following conditions: a flow rate of 2 mL h^{-1}, an

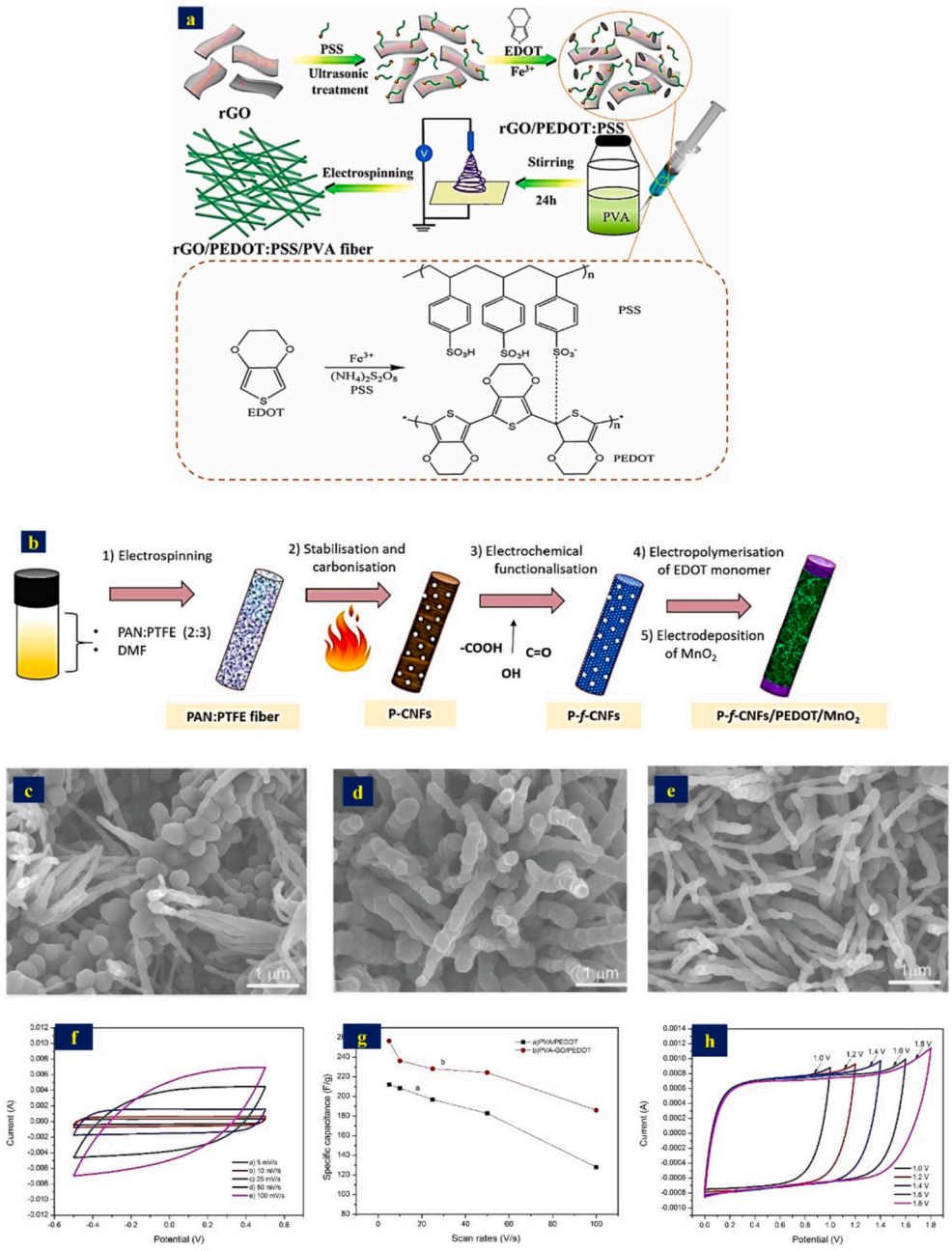

Fig. 10. (a) Typical representation of the preparative procedure for PEDOT: PSS/RGO/PVA fiber-based composite electrode through ultrasonic, electropolymerization, and ES processes, the EDOT electropolymerization equation is provided below the schematic diagram, reproduced with permission from Ref [144], (b) graphical representation of the construction of PEDOT/MnO_2/f-PCNFs fiber composite positive electrode for flexible SCs, reproduced with permission from Ref [145], (c–e) change in surface morphology of PEDOT fibers with respect to vapor polymerization times, (c) low vapor polymerization time, (d) medium vapor polymerization time, and (e) high vapor polymerization time, reproduced with permission from Ref [146], (f) CV profile of PEDOT/PVA-GO at various scan rates ranging from 5 to 100 mV s^{-1}, (g) determined specific capacitance as the function of scan rate for both pristine and composite electrodes, and (h) CV plot of the composite electrode at the constant potential of 20 mV s^{-1} at various potential windows from 1 to 1.8 V, reproduced with permission from Ref [147].

applied potential of 15 kV, and a rotation speed of 8 s/r [152]. The resultant electrode possesses a porous fibrous morphology with excellent electrochemical properties, such as capacitance of 188.5 F cm^{-3} and 80 % retention even after 1.9 million GCD cycles. On the other hand, the sonication processed PEDOT/Nafion provides a rough, thin surface morphology at room temperature [153]. It yields the maximum capacitance of 74 F cm^{-3} with a capacitance retention of 98.7 % over 1000 cycles.

In conclusion, PEDOT has emerged as a leading conducting polymer due to its exceptional electrical conductivity, environmental stability, processability, and diverse applications. Its unique combination of properties has unlocked new possibilities in organic electronics, paving the way for developing advanced technologies such as flexible displays, wearable devices, energy storage systems, and more. With ongoing research and innovation, PEDOT is promising for future materials science and technology advancements.

4. Conclusion and future perspectives

This work systematically reviews binder-free, flexible, self-standing CPs-derived nanofiber electrodes through the ES process for high-performance SCs. A brief discussion on the electrochemical

evaluations and properties of the SCs is demonstrated. The reviewed literature displays the fundamental objective of the ES process for constructing CNFs with high SSA and low density for improved electrochemical supercapacitive performance. In addition, electrospun CNFs offer excellent beneficial properties, including the ability to develop binder-free materials and the potential to accommodate other active compounds, leading to improved electrochemical performance. Moreover, electrospun CNFs exhibit outstanding electrical conductivity, flexibility, and high mechanical strength, enabling rapid electron transfer and improving the electrodes' overall conductivity, durability, and structural stability. Due to the specific characteristics of CNFs, they may create a self-standing electrode that affords a large amount of electrolytes and reduces the ion-migration pathways. Further, the exceptional flexibility of these fibrous electrodes provides better performance under bending conditions due to less fracture over the electrode surface.

Despite their advantages, CNF-based electrodes also have certain limitations. While CNFs are becoming more cost-effective, their production can still be relatively expensive compared to conventional electrode materials. Moreover, achieving precise control over the properties of CNF-based electrodes can be challenging and may require optimizing processing parameters. Constructing CNF-based electrodes may face critical challenges like scalability and long-term stability. Continual refinement and optimization of fabrication processes can improve control over properties and enhance reproducibility. Exploring new precursor materials or composites, such as functionalized CNFs or hybrid structures, can improve performance and overcome limitations. The structure and electrochemical properties of CNF-based electrodes can be improved through various strategies, such as doping and hybridization with other materials. Introducing dopants or functional groups onto CNFs can modify their electrochemical properties, such as enhancing specific capacitance or stability. Incorporating additional materials, such as metal oxides, CPs, or carbon nanomaterials, into CNF-based electrodes can improve their electrochemical performance.

CPs such as PANI, PPy, PTh, and PEDOT have gained huge attention in advanced EES devices, especially in high-performance asymmetric SCs. These CPs possess excellent characteristics, including high conductivity, facile production, redox properties, cost-effectiveness, and eco-stability, making them potential candidates for high-performance SCs. Incorporating CPs such as PANI, PPy, PTh, and PEDOT, individually or in association with other compounds, shows these materials' flexibility and potential ability in advanced EES devices. With the increasing dominance of portable electronics, the importance of their energy density and flexibility is ever-increasing. Recent studies indicate that the high-performance SCs based on these CPs exhibit more specific capacitance than other electrodes, suggesting improved electrical charge storage ability. In addition, CPs-based electrospun CNFs provide extremely prolonged electrochemical cycling stability, highlighting their durability over many GCD cycles. Asymmetric SCs based on CPs-based CNFs show high energy and power densities, implying their ability to preserve large energy per unit mass.

CPs-based CNFs have several uses in hybrid, symmetric, and asymmetric SCs, although they comprise many disputes. Using these electrodes during the GCD process provides a sudden decrement in capacitance, which might be attributed to the mechanical deterioration of CPs. Mechanical fragility is one of the important drawbacks of CPs-based CNFs when employed over a prolonged time, which exhibits variable conductivity during the electrochemical process. Even though the CPs-based CNFs possess high power density, their energy density is relatively lower than that of conventional electrode materials. In addition, structural instability is one of the major concerns for CPs, which is generated by volume expansion during the redox electrochemical process. Due to compatibility problems with several electrolytes, the operational conditions of these electrode materials are limited. Henceforth, it is essential to develop alternate methods to improve the overall performance of CPs-based CNFs in high-performance SCs.

SCs have numerous potential applications, from transportation to electronics to medical devices. Ongoing research is focused on improving their performance, reducing their cost, and developing new and innovative applications for this promising technology. We firmly trust that implementing alternate secondary strategies and technologies could overcome the drawbacks of pure electrospun CNFs in EES devices. As such, SCs will likely continue to play an important role in fields like flexible and wearable devices, hybrid energy storage systems, and the development of sustainable and efficient energy systems in the future. Researching the impacts of surface modifications and morphological alterations on the electrochemical performance of CPs-based CNFs-based SCs is crucial for determining the most favorable design parameters to achieve improved efficiency. Next-generation research must focus on structural deterioration, electrolyte dissolution, and capacity loss in SCs. Stable binders, improved electrolytes, and protective coatings can enhance long-term cyclability and stability. Other broad synthesis methods and roll-to-roll processing of these electrodes can cost-effectively create flexible and lightweight electronics. By developing the possibility of combining CPs with other materials and new device architectures, multifunctional EES devices that may be used in various applications can be created. Overall, this review explains the CPs-derived electrospun CNFs-based electrode materials employed so far and gives a complete insight into the future advancement of high-performance SCs for electronic devices.

CRediT authorship contribution statement

Jining Lin: Writing – original draft, Investigation, Formal analysis, Data curation. **K. Karuppasamy:** Writing – review & editing, Writing – original draft, Validation, Methodology, Investigation, Data curation, Conceptualization. **Ranjith Bose:** Writing – original draft, Resources, Investigation. **Dhanasekaran Vikraman:** Writing – original draft, Validation, Investigation. **Saeed Alameri:** Writing – review & editing, Visualization, Validation, Resources. **T. Maiyalagan:** Writing – original draft, Validation, Resources. **Hyun-Seok Kim:** Writing – review & editing, Validation, Resources, Methodology. **Akram Alfantazi:** Writing – review & editing, Validation, Supervision. **Jan G. Korvink:** Writing – review & editing, Writing – original draft, Validation, Supervision. **Bharat Sharma:** Writing – review & editing, Writing – original draft, Validation, Resources, Conceptualization.

Declaration of competing interest

The authors declare that they have no known competing financial interests or personal relationships that could have appeared to influence the work reported in this paper.

Data availability

Data will be made available on request.

Acknowledgments

This work was partly supported by the Deutsche Forschungsgemeinschaft (DFG, German Research Foundation) under Germany's Excellence Strategy via the Excellence Cluster *3D Matter Made to Order* (EXC-2082/1-390761711). One of the authors, Dr. K. K., thankfully acknowledges Khalifa University of Science, Technology and Research, Abu Dhabi, for the funding support.

References

[1] Y. Yang, T. Zhu, L. Shen, Y. Liu, D. Zhang, B. Zheng, K. Gong, J. Zheng, X. Gong, Recent progress in the all-solid-state flexible supercapacitors, SmartMat 3 (2022) 349–383.

[2] C. Xiong, T. Wang, Z. Zhao, Y. Ni, Recent progress in the development of smart supercapacitors, SmartMat 4 (2023) e1158.

[3] S. Keshavarz, O.V. Okoro, M. Hamidi, H. Derakhshankhah, M. Azizi, S. Mohammad Nabavi, S. Gholizadeh, S.M. Amini, A. Shavandi, R. Luque, H. Samadian, Synthesis, surface modifications, and biomedical applications of carbon nanofibers: electrospun vs vapor-grown carbon nanofibers, Coord. Chem. Rev. 472 (2022) 214770.

[4] M. Pandey, K. Deshmukh, A. Raman, A. Asok, S. Appukuttan, G.R. Suman, Prospects of MXene and graphene for energy storage and conversion, Renew. Sust. Energ. Rev. 189 (2024) 114030.

[5] S. Ramesh, K. Karuppasamy, D. Vikraman, E. Kim, L. Sanjeeb, Y.-J. Lee, H.-S. Kim, J.-H. Kim, H.S. Kim, Hierarchical Co3O4 decorated nitrogen-doped graphene oxide nanosheets for energy storage and gas sensing applications, J. Ind. Eng. Chem. 101 (2021) 253–261.

[6] K. Karuppasamy, D. Vikraman, R. Bose, S. Hussain, P. Santhoshkumar, R. Manikandan, J. Jung, S. Alameri, A. Alfantazi, H.-S. Kim, Unveiling the redox electrochemical kinetics of interconnected wrinkled microspheres of binary Cu2-xSe/Ni1-xSe as battery-type electrode for advanced supercapatteries, J. Colloid Interface Sci. 654 (2024) 1098–1110.

[7] B. Yan, W. Zhao, Q. Zhang, Q. Kong, G. Chen, C. Zhang, J. Han, S. Jiang, S. He, One stone for four birds: a "chemical blowing" strategy to synthesis wood-derived carbon monoliths for high-mass loading capacitive energy storage in low temperature, J. Colloid Interface Sci. 653 (2024) 1526–1538.

[8] Y. Zhao, Y. Zhang, Y. Wang, D. Cao, X. Sun, H. Zhu, Versatile zero- to three-dimensional carbon for electrochemical energy storage, Carbon, Energy 3 (2021) 895–915.

[9] J. Pu, Y. Gao, Q. Cao, G. Fu, X. Chen, Z. Pan, C. Guan, Vanadium metal-organic framework-derived multifunctional fibers for asymmetric supercapacitor, piezoresistive sensor, and electrochemical water splitting, SmartMat 3 (2022) 608–618.

[10] T. Yue, B. Shen, P. Gao, Carbon material/MnO2 as conductive skeleton for supercapacitor electrode material: a review, Renew. Sust. Energ. Rev. 158 (2022) 112131.

[11] Q. Kong, Q. Zhang, B. Yan, J. Chen, D. Chen, L. Jiang, T. Lan, C. Zhang, W. Yang, S. He, N/O co-doped porous carbon synthesized by Lewis acid salt activation for high rate performance supercapacitor, Journal of Energy Storage 80 (2024) 110322.

[12] F.-F. Sun, W.-H. Li, Z.-H. Huang, W. Sun, Y. Dou, D. Yuan, B. Jia, T. Ma, Pulse-potential electrochemistry to boost real-life application of pseudocapacitive dual-doped polypyrrole, SmartMat 3 (2022) 644–656.

[13] H. Wang, C. Wang, Y. Tang, Interface engineering toward high-efficiency alloy anode for next-generation energy storage device, EcoMat 3 (2021) e12172.

[14] J. Chu, Y. Wang, F. Zhong, X. Feng, W. Chen, X. Ai, H. Yang, Y. Cao, Metal/covalent-organic frameworks for electrochemical energy storage applications, EcoMat 3 (2021) e12133.

[15] K. Krishnamoorthy, P. Pazhamalai, S. Manoharan, N.U.H. Liyakath Ali, S.-J. Kim, Recent trends, challenges, and perspectives in piezoelectric-driven self-chargeable electrochemical supercapacitors, Carbon, Energy 4 (2022) 833–855.

[16] N. Lingappan, W. Lee, S. Passerini, M. Pecht, A comprehensive review of separator membranes in lithium-ion batteries, Renew. Sust. Energ. Rev. 187 (2023) 113726.

[17] R.T. Yadlapalli, R.R. Alla, R. Kandipati, A. Kotapati, Super capacitors for energy storage: progress, applications and challenges, Journal of Energy Storage 49 (2022) 104194.

[18] J. Zhao, A.F. Burke, Electrochemical capacitors: materials, technologies and performance, Energy Storage Materials 36 (2021) 31–55.

[19] W. Chen, K. Yang, M. Luo, D. Zhang, Z. Li, C. Liu, X. Zhou, Carbonization-free wood electrode with MXene-reconstructed porous structure for all-wood eco-supercapacitors, EcoMat 5 (2023) e12271.

[20] Z. Shang, X. An, S. Nie, N. Li, H. Cao, Z. Cheng, H. Liu, Y. Ni, L. Liu, Design of B/N Co-doped micro/meso porous carbon electrodes from CNF/BNNS/ZIF-8 nanocomposites for advanced supercapacitors, Journal of Bioresources and Bioproducts 8 (2023) 292.

[21] P. Xie, W. Yuan, X. Liu, Y. Peng, Y. Yin, Y. Li, Z. Wu, Advanced carbon nanomaterials for state-of-the-art flexible supercapacitors, Energy Storage Materials 36 (2021) 56–76.

[22] R.A. Perera Jayawickramage, K.J. Balkus, J.P. Ferraris, Binder free carbon nanofiber electrodes derived from polyacrylonitrile-lignin blends for high performance supercapacitors, Nanotechnology 30 (2019) 355402.

[23] N.C. Abeykoon, V. Garcia, R.A. Jayawickramage, W. Perera, J. Cure, Y.J. Chabal, K.J. Balkus, J.P. Ferraris, Novel binder-free electrode materials for supercapacitors utilizing high surface area carbon nanofibers derived from immiscible polymer blends of PBI/6FDA-DAM:DABA, RSC Adv. 7 (2017) 20947–20959.

[24] R. Xu, L. Du, D. Adekoya, G. Zhang, S. Zhang, S. Sun, Y. Lei, Well-defined nanostructures for electrochemical energy conversion and storage, Adv. Energy Mater. 11 (2021) 2001537.

[25] Z. Qiao, M. Shen, Y. Xiao, M. Zhu, S. Mignani, J.-P. Majoral, X. Shi, Organic/inorganic nanohybrids formed using electrospun polymer nanofibers as nanoreactors, Coord. Chem. Rev. 372 (2018) 31–51.

[26] R. Shaik, R.K. Kampara, A. Kumar, C.S. Sharma, M. Kumar, Metal oxide nanofibers based chemiresistive H2S gas sensors, Coord. Chem. Rev. 471 (2022) 214752.

[27] R. Gusain, N. Kumar, S.S. Ray, Recent advances in carbon nanomaterial-based adsorbents for water purification, Coord. Chem. Rev. 405 (2020) 213111.

[28] B. Joshi, E. Samuel, Y.-I. Kim, A.L. Yarin, M.T. Swihart, S.S. Yoon, Review of recent progress in electrospinning-derived freestanding and binder-free electrodes for supercapacitors, Coord. Chem. Rev. 460 (2022) 214466.

[29] W. Lei, H. Li, Y. Tang, H. Shao, Progress and perspectives on electrospinning techniques for solid-state lithium batteries, Carbon, Energy 4 (2022) 539–575.

[30] W. Cai, Y. Zhang, Y. Jia, J. Yan, Flexible heteroatom-doped porous carbon nanofiber cages for electrode scaffolds, Carbon, Energy 2 (2020) 472–481.

[31] D. Han, A.J. Steckl, Coaxial electrospinning formation of complex polymer fibers and their applications, ChemPlusChem 84 (2019) 1453–1497.

[32] Z. Zhao, Y. Miao, Q. Lu, Electrospun nickel cobalt phosphide/carbon nanofibers as high-performance electrodes for supercapacitors, J. Power Sources 606 (2024) 234587.

[33] B. Joshi, E. Samuel, Y.-I. Kim, A.L. Yarin, M.T. Swihart, S.S. Yoon, Progress and potential of electrospinning-derived substrate-free and binder-free lithium-ion battery electrodes, Chem. Eng. J. 430 (2022) 132876.

[34] J. Theerthagiri, A.P. Murthy, S.J. Lee, K. Karuppasamy, S.R. Arumugam, Y. Yu, M. M. Hanafiah, H.-S. Kim, V. Mittal, M.Y. Choi, Recent progress on synthetic strategies and applications of transition metal phosphides in energy storage and conversion, Ceram. Int. 47 (2021) 4404–4425.

[35] D. Vikraman, S. Hussain, K. Karuppasamy, A. Feroze, A. Kathalingam, A. Sanmugam, S.-H. Chun, J. Jung, H.-S. Kim, Engineering the novel MoSe2-Mo2C hybrid nanoarray electrodes for energy storage and water splitting applications, Applied Catalysis B: Environmental 264 (2020) 118531.

[36] I. Rabani, K. Karuppasamy, D. Vikraman, Z. Ul Haq, H.-S. Kim, Y.-S. Seo, Hierarchical structured nano-polyhedrons of CeO2@ZIF-8 composite for high performance supercapacitor applications, J. Alloys Compd. 875 (2021) 160074.

[37] I. Rabani, J. Yoo, H.-S. Kim, D.V. Lam, S. Hussain, K. Karuppasamy, Y.-S. Seo, Highly dispersive Co3O4 nanoparticles incorporated into a cellulose nanofiber for a high-performance flexible supercapacitor, Nanoscale 13 (2021) 355–370.

[38] S. Ramesh, K. Karuppasamy, H.-S. Kim, H.S. Kim, J.-H. Kim, Hierarchical flowerlike 3D nanostructure of Co3O4@MnO2/N-doped graphene oxide (NGO) hybrid composite for a high-performance supercapacitor, Sci. Rep. 8 (2018) 16543.

[39] P. Khamnantha, C. Homla-or, K. Suttisintong, J. Manyam, M. Raita, V. Champreda, V. Intasanta, H.-J. Butt, R. Berger, A. Pangon, Stable lignin-rich nanofibers for binder-free carbon electrodes in supercapacitors, ACS Applied Nano Materials 4 (2021) 13099–13111.

[40] B. Zhang, F. Kang, J.-M. Tarascon, J.-K. Kim, Recent advances in electrospun carbon nanofibers and their application in electrochemical energy storage, Prog. Mater. Sci. 76 (2016) 319–380.

[41] J.-H. Liu, P. Wang, Z. Gao, X. Li, W. Cui, R. Li, S. Ramakrishna, J. Zhang, Y.-Z. Long, Review on electrospinning anode and separators for lithium ion batteries, Renew. Sust. Energ. Rev. 189 (2024) 113939.

[42] N. Haleem, A. Khattak, Y. Jamal, M. Sajid, Z. Shahzad, H. Raza, Development of poly vinyl alcohol (PVA) based biochar nanofibers for carbon dioxide (CO2) adsorption, Renew. Sust. Energ. Rev. 157 (2022) 112019.

[43] F. Xie, L. Sun, J. Qian, X. Shi, J. Hu, Y. Qu, H. Tan, K. Wang, Y. Zhang, Polypyrrole-coated boron-doped nickel-cobalt sulfide on electrospinning carbon nanofibers for high performance asymmetric supercapacitors, J. Colloid Interface Sci. 628 (2022) 371–383.

[44] D. Wang, Y. Lian, H. Fu, Q. Zhou, Y. Zheng, H. Zhang, Flexible porous carbon nanofibers derived from cuttlefish ink as self-supporting electrodes for supercapacitors, J. Power Sources 599 (2024) 234216.

[45] S. Peng, L. Li, J. Kong Yoong Lee, L. Tian, M. Srinivasan, S. Adams, S. Ramakrishna, Electrospun carbon nanofibers and their hybrid composites as advanced materials for energy conversion and storage, Nano Energy 22 (2016) 361–395.

[46] J. Liang, H. Zhao, L. Yue, G. Fan, T. Li, S. Lu, G. Chen, S. Gao, Abdullah M. Asiri, X. Sun, Recent advances in electrospun nanofibers for supercapacitors, J. Mater. Chem. A 8 (2020) 16747–16789.

[47] C. Ma, G. Song, Z. Li, H. Wu, C. Wang, Y. Wang, X. Zhang, Y. Song, J. Shi, High-areal-capacitance electrode constructed by lignin-based microporous carbon nanofibers for supercapacitors, Journal of Energy Storage 88 (2024) 111465.

[48] S. Roy, P. Panda, S. Barman, Electrospun highly porous carbon nitride-carbon nanofibers for high performance supercapacitor application, Journal of Energy Storage 91 (2024) 112007.

[49] D. Wang, K. Tang, J. Xiao, X. Li, M. Long, J. Chen, H. Gao, W. Chen, C. Liu, H. Liu, Advances of electrospun Mo-based nanocomposite fibers as anode materials for supercapacitors, Sustain. Mater. Technol. 29 (2021) e00302.

[50] S.N. Banitaba, A. Ehrmann, Application of electrospun nanofibers for fabrication of versatile and highly efficient electrochemical devices: a review, Polymers 13 (2021) 1741.

[51] H. Wang, H. Wang, R. Sun, L. Yao, H. Zuo, F. Ruan, Q. Feng, J. Wang, Preparation of hierarchical micro-meso porous carbon and carbon nanofiber from polyacrylonitrile/polysulfone polymer via one-step carbonization for supercapacitor electrodes, Electrochim. Acta 441 (2023) 141827.

[52] S. Sardana, A. Gupta, K. Singh, A.S. Maan, A. Ohlan, Conducting polymer hydrogel based electrode materials for supercapacitor applications, Journal of Energy Storage 45 (2022) 103510.

[53] Z. Zhao, L. Sun, Y. Li, W. Feng, Polymer-derived carbon materials for energy storage devices: a mini review, Carbon 210 (2023) 118066.

[54] A. Haider, S. Haider, I.-K. Kang, A comprehensive review summarizing the effect of electrospinning parameters and potential applications of nanofibers in biomedical and biotechnology, Arab. J. Chem. 11 (2018) 1165–1188.

[55] H. Fong, I. Chun, D.H. Reneker, Beaded nanofibers formed during electrospinning, Polymer 40 (1999) 4585–4592.

[56] I.B. Rietveld, K. Kobayashi, H. Yamada, K. Matsushige, Electrospray deposition, model, and experiment: toward general control of film morphology, J. Phys. Chem. B 110 (2006) 23351–23364.

[57] Z. Jiang, X. Yu, Understanding of droplet dynamics and deposition area in electrospraying process: modeling and experimental Approaches, arXiv preprint arXiv:1809.09688, (2018).
[58] E. Ewaldz, J. Randrup, B. Brettmann, Solvent effects on the elasticity of electrospinnable polymer solutions, ACS Polymers Au 2 (2022) 108–117.
[59] S. Hao, X. Sheng, F. Xie, M. Sun, F. Diao, Y. Wang, Electrospun carbon nanofibers embedded with heterostructured NiFe2O4/Fe0.64Ni0.36 nanoparticles as an anode for high-performance lithium-ion battery, Journal of Energy Storage 80 (2024) 110412.
[60] M. Inagaki, Y. Yang, F. Kang, Carbon nanofibers prepared via electrospinning, Adv. Mater. 24 (2012) 2547–2566.
[61] D. Li, Y. Wang, Y. Xia, Electrospinning of polymeric and ceramic nanofibers as uniaxially aligned arrays, Nano Lett. 3 (2003) 1167–1171.
[62] H. Gao, B. Joshi, E. Samuel, A. Khadka, S. Wung Kim, A. Aldalbahi, M. El-Newehy, S.S. Yoon, Freestanding electrodes based on nitrogen-doped carbon nanofibers and zeolitic imidazolate framework-derived ZnO for flexible supercapacitors, Appl. Surf. Sci. 651 (2024) 159221.
[63] N.E. Zander, Hierarchically structured electrospun fibers, Polymers (2013) 19–44.
[64] H.-N. Jang, M.-H. Jo, H.-J. Ahn, Tailored functional group vitalization on mesoporous carbon nanofibers for ultrafast electrochemical capacitors, Appl. Surf. Sci. 623 (2023) 157081.
[65] Z. Ayaganov, V. Pavlenko, S.F.B. Haque, A. Tanybayeva, J. Ferraris, A. Zakhidov, Z. Mansurov, Z. Bakenov, A. Ng, A comprehensive study on effect of carbon nanomaterials as conductive additives in EDLCs, Journal of Energy Storage 78 (2024) 110035.
[66] D. Kim, T.G. Yun, J.H. Lee, K.R. Yoon, K. Kim, Rational design of conductive metal–organic frameworks and aligned carbon nanofibers for enhancing the performance of flexible supercapacitors, Nanoscale Advances 6 (2024) 1900–1908.
[67] M.M. Sk, P. Pradhan, B.K. Patra, A.K. Guria, Green biomass derived porous carbon materials for electrical double-layer capacitors (EDLCs), Materials Today Chemistry 30 (2023) 101582.
[68] A.R. Peringath, M.A.H. Bayan, M. Beg, A. Jain, F. Pierini, N. Gadegaard, R. Hogg, L. Manjakkal, Chemical synthesis of polyaniline and polythiophene electrodes with excellent performance in supercapacitors, Journal of Energy Storage 73 (2023) 108811.
[69] M. Sadiq, M.A. Khan, M. Sarvar, M.M.H. Raza, S.M. Aalam, M. Zulfequar, J. Ali, High electrochemical performance of rGO-CNTs composites as an electrode material for supercapacitors applications, Hybrid Advances 3 (2023) 100051.
[70] S.H. Kang, G.Y. Lee, J. Lim, S.O. Kim, CNT–rGO hydrogel-integrated fabric composite synthesized via an interfacial gelation process for wearable supercapacitor electrodes, ACS Omega 6 (2021) 19578–19585.
[71] M.A.A. Mohd Abdah, N.H.N. Azman, S. Kulandaivalu, Y. Sulaiman, Review of the use of transition-metal-oxide and conducting polymer-based fibres for high-performance supercapacitors, Mater. Des. 186 (2020) 108199.
[72] A. Tundwal, H. Kumar, B.J. Binoj, R. Sharma, G. Kumar, R. Kumari, A. Dhayal, A. Yadav, D. Singh, P. Kumar, Developments in conducting polymer-, metal oxide-, and carbon nanotube-based composite electrode materials for supercapacitors: a review, RSC Adv. 14 (2024) 9406–9439.
[73] M. Naveed ur Rehman, T. Munawar, M.S. Nadeem, F. Mukhtar, A. Maqbool, M. Riaz, S. Manzoor, M.N. Ashiq, F. Iqbal, Facile synthesis and characterization of conducting polymer-metal oxide based core-shell PANI-Pr2O–NiO–Co3O4 nanocomposite: as electrode material for supercapacitor, Ceram. Int. 47 (2021) 18497–18509.
[74] W. Wang, J. Cao, J. Yu, F. Tian, X. Luo, Y. Hao, J. Huang, F. Wang, W. Zhou, J. Xu, X. Liu, H. Yang, Flexible supercapacitors based on stretchable conducting polymer electrodes, Polymers 15 (2023) 1856.
[75] S. Wustoni, D. Ohayon, A. Hermawan, A. Nuruddin, S. Inal, Y.S. Indartono, B. Yuliarto, Material design and characterization of conducting polymer-based supercapacitors, Polym. Rev. 64 (2024) 192–250.
[76] Y. Liu, F. Wu, Synthesis and application of polypyrrole nanofibers: a review, Nanoscale Adv. 5 (2023) 3606–3618.
[77] P. Yang, W. Mai, Flexible solid-state electrochemical supercapacitors, Nano Energy 8 (2014) 274–290.
[78] C. Weidlich, K.M. Mangold, K. Jüttner, EQCM study of the ion exchange behaviour of polypyrrole with different counterions in different electrolytes, Electrochim. Acta 50 (2005) 1547–1552.
[79] M. Ates, Y. Yuruk, Facile preparation of reduced graphene oxide, polypyrrole, carbon black, and polyvinyl alcohol nanocomposite by electrospinning: a low-cost and sustainable approach for supercapacitor application, Ionics 27 (2021) 2659–2672.
[80] G. Nie, X. Lu, M. Chi, Y. Jiang, C. Wang, CoOx nanoparticles embedded in porous graphite carbon nanofibers derived from electrospun polyacrylonitrile@polypyrrole core–shell nanostructures for high-performance supercapacitors, RSC Adv. 6 (2016) 54693–54701.
[81] A.-W. Chai, C.-C. Wang, C.-Y. Chen, Synthesis and characterization of modified centrifuged-electrospun carbon nanofibers for high-performance supercapacitor electrodes, J. Taiwan Inst. Chem. Eng. 156 (2024) 105329.
[82] M. Shao, Z. Li, R. Zhang, F. Ning, M. Wei, D.G. Evans, X. Duan, Hierarchical conducting polymer@clay core–shell arrays for flexible all-solid-state supercapacitor devices, Small 11 (2015) 3530–3538.
[83] S. Ramesh, H.M. Yadav, K. Karuppasamy, D. Vikraman, H.-S. Kim, J.-H. Kim, H. S. Kim, Fabrication of manganese oxide@nitrogen doped graphene oxide/polypyrrole (MnO2@NGO/PPy) hybrid composite electrodes for energy storage devices, J. Mater. Res. Technol. 8 (2019) 4227–4238.
[84] Y. Huang, H. Li, Z. Wang, M. Zhu, Z. Pei, Q. Xue, Y. Huang, C. Zhi, Nanostructured Polypyrrole as a flexible electrode material of supercapacitor, Nano Energy 22 (2016) 422–438.
[85] L. Chen, D. Li, L. Chen, P. Si, J. Feng, L. Zhang, Y. Li, J. Lou, L. Ci, Core-shell structured carbon nanofibers yarn@polypyrrole@graphene for high performance all-solid-state fiber supercapacitors, Carbon 138 (2018) 264–270.
[86] L. Chen, L. Chen, Q. Ai, D. Li, P. Si, J. Feng, L. Zhang, Y. Li, J. Lou, L. Ci, Flexible all-solid-state supercapacitors based on freestanding, binder-free carbon nanofibers@polypyrrole@graphene film, Chem. Eng. J. 334 (2018) 184–190.
[87] R. Mahore, D. Burghate, P. Burghate, S. Kondawar, P. Patil, B. Meshram, Fabrication of Electrospun Nanofibers of Ternary Composite Polypyrrole-CNT-MnO2.
[88] Y.-S. Sung, L.-Y. Lin, Systematic design of polypyrrole/carbon fiber electrodes for efficient flexible fiber-type solid-state supercapacitors, Nanomaterials 10 (2020) 248.
[89] Y. Wang, S. Gan, J. Meng, J. Yang, J. Li, H. Liu, L. Shi, L. Chen, Layered nanofiber yarn for high-performance flexible all-solid supercapacitor electrodes, J. Phys. Chem. C 125 (2021) 1190–1199.
[90] X. Lu, C. Wang, F. Favier, N. Pinna, Electrospun nanomaterials for supercapacitor electrodes: designed architectures and electrochemical performance, Adv. Energy Mater. 7 (2017) 1601301.
[91] W. Xiong, X. Hu, X. Wu, Y. Zeng, B. Wang, G. He, Z. Zhu, A flexible fiber-shaped supercapacitor utilizing hierarchical NiCo2O4@polypyrrole core–shell nanowires on hemp-derived carbon, J. Mater. Chem. A 3 (2015) 17209–17216.
[92] Y. Song, T.-Y. Liu, X.-X. Xu, D.-Y. Feng, Y. Li, X.-X. Liu, Pushing the cycling stability limit of polypyrrole for supercapacitors, Adv. Funct. Mater. 25 (2015) 4626–4632.
[93] K. Liang, T. Gu, Z. Cao, X. Tang, W. Hu, B. Wei, In situ synthesis of SWNTs@MnO2/polypyrrole hybrid film as binder-free supercapacitor electrode, Nano Energy 9 (2014) 245–251.
[94] Y. Shi, L. Pan, B. Liu, Y. Wang, Y. Cui, Z. Bao, G. Yu, Nanostructured conductive polypyrrole hydrogels as high-performance, flexible supercapacitor electrodes, J. Mater. Chem. A 2 (2014) 6086–6091.
[95] J. Tao, N. Liu, W. Ma, L. Ding, L. Li, J. Su, Y. Gao, Solid-state high performance flexible supercapacitors based on polypyrrole-MnO2-carbon fiber hybrid structure, Sci. Rep. 3 (2013) 2286.
[96] R. Xu, F. Guo, X. Cui, L. Zhang, K. Wang, J. Wei, High performance carbon nanotube based fiber-shaped supercapacitors using redox additives of polypyrrole and hydroquinone, J. Mater. Chem. A 3 (2015) 22353–22360.
[97] J. Zhu, Y. Xu, J. Wang, J. Wang, Y. Bai, X. Du, Morphology controllable nanosheet polypyrrole–graphene composites for high-rate supercapacitor, Phys. Chem. Chem. Phys. 17 (2015) 19885–19894.
[98] Y. Huang, J. Tao, W. Meng, M. Zhu, Y. Huang, Y. Fu, Y. Gao, C. Zhi, Super-high rate stretchable polypyrrole-based supercapacitors with excellent cycling stability, Nano Energy 11 (2015) 518–525.
[99] Y. Huang, M. Zhu, W. Meng, Y. Fu, Z. Wang, Y. Huang, Z. Pei, C. Zhi, Robust reduced graphene oxide paper fabricated with a household non-stick frying pan: a large-area freestanding flexible substrate for supercapacitors, RSC Adv. 5 (2015) 33981–33989.
[100] X. Sun, Y. Jin, C.-Y. Zhang, J.-W. Wen, Y. Shao, Y. Zang, C.-H. Chen, Na[Ni0.4Fe0.2Mn0.4−xTix]O2: a cathode of high capacity and superior cyclability for Na-ion batteries, J. Mater. Chem. A 2 (2014) 17268–17271.
[101] C. Yang, J. Shen, C. Wang, H. Fei, H. Bao, G. Wang, All-solid-state asymmetric supercapacitor based on reduced graphene oxide/carbon nanotube and carbon fiber paper/polypyrrole electrodes, J. Mater. Chem. A 2 (2014) 1458–1464.
[102] A.V. Salkar, S.V. Bhosale, P.P. Morajkar, 6-Nanostructured WO3−x based advanced supercapacitors for sustainable energy applications, in: S.D. Delekar (Ed.), Advances in Metal Oxides and Their Composites for Emerging Applications, Elsevier, 2022, pp. 213–238.
[103] Y. Song, M. Shang, J. Li, Y. Su, Continuous and controllable synthesis of MnO2/PPy composites with core–shell structures for supercapacitors, Chem. Eng. J. 405 (2021) 127059.
[104] G. Zhang, W. Cao, H. Zhang, Y. Hou, J. Guo, Facial synthesis of Fe3O4/PPy core–shell composite electrode material for boosted supercapacity, Energy Fuel 36 (2022) 5018–5026.
[105] C. Fu, H. Zhou, R. Liu, Z. Huang, J. Chen, Y. Kuang, Supercapacitor based on electropolymerized polythiophene and multi-walled carbon nanotubes composites, Mater. Chem. Phys. 132 (2012) 596–600.
[106] A. Shokry, M. Karim, M. Khalil, S. Ebrahim, J. El Nady, Supercapacitor based on polymeric binary composite of polythiophene and single-walled carbon nanotubes, Sci. Rep. 12 (2022) 11278.
[107] A. Alabadi, S. Razzaque, Z. Dong, W. Wang, B. Tan, Graphene oxide-polythiophene derivative hybrid nanosheet for enhancing performance of supercapacitor, J. Power Sources 306 (2016) 241–247.
[108] Y. Li, M. Zhou, Y. Wang, Q. Pan, Q. Gong, Z. Xia, Y. Li, Remarkably enhanced performances of novel polythiophene-grafting-graphene oxide composite via long alkoxy linkage for supercapacitor application, Carbon 147 (2019) 519–531.
[109] B. Chen, W.-Y. Wong, Introducing a redox-active ferrocenyl moiety onto a polythiophene derivative towards high-performance flexible all-solid-state symmetric supercapacitors, J. Mater. Chem. A 10 (2022) 7968–7977.
[110] X. Hong, Y. Liu, Y. Li, X. Wang, J. Fu, X. Wang, Application progress of polyaniline, polypyrrole and polythiophene in lithium-sulfur batteries, Polymers 12 (2020) 331.
[111] M. Mohammadizadeh, A.A. Yousefi, Deposition of conductive polythiophene film on a piezoelectric substrate: effect of corona poling and nano-inclusions, Iran. Polym. J. 25 (2016) 415–422.

[112] R.B. Ambade, S.B. Ambade, N.K. Shrestha, R.R. Salunkhe, W. Lee, S.S. Bagde, J. H. Kim, F.J. Stadler, Y. Yamauchi, S.-H. Lee, Controlled growth of polythiophene nanofibers in TiO2 nanotube arrays for supercapacitor applications, J. Mater. Chem. A 5 (2017) 172–180.
[113] A.K. Thakur, M. Majumder, R.B. Choudhary, S.N. Pimpalkar, Supercapacitor based on electropolymerized polythiophene and multiwalled carbon nanotubes composites, IOP Conference Series: Materials Science and Engineering 149 (2016) 012166.
[114] N.N. Maşlakci, Electrospun polyacrylonitrile/polythiophene fibers for phosphate anion sensing, Bilge International Journal of Science and Technology Research (2020) 6–12.
[115] M. Azimi, M. Abbaspour, A. Fazli, H. Setoodeh, B. Pourabbas, Investigation on electrochemical properties of polythiophene nanocomposite with graphite derivatives as supercapacitor material on breath figure-decorated PMMA electrode, J. Electron. Mater. 47 (2018) 2093–2102.
[116] A.u. Rahman, H. Noreen, Z. Nawaz, J. Iqbal, G. Rahman, M. Yaseen, Synthesis of graphene nanoplatelets/polythiophene as a high performance supercapacitor electrode material, New J. Chem. 45 (2021) 16187–16195.
[117] Q. Meng, K. Cai, Y. Chen, L. Chen, Research progress on conducting polymer based supercapacitor electrode materials, Nano Energy 36 (2017) 268–285.
[118] W. Matysiak, T. Tański, W. Smok, K. Gołombek, E. Schab-Balcerzak, Effect of conductive polymers on the optical properties of electrospun polyacrylonitryle nanofibers filled by polypyrrole, polythiophene and polyaniline, Appl. Surf. Sci. 509 (2020) 145068.
[119] Z.H. Momin, A.T.A. Ahmed, D.D. Malkhede, J.R. Koduru, Synthesis of thin-film composite of MWCNTs-polythiophene-Ru/Pd at liquid-liquid interface for supercapacitor application, Inorg. Chem. Commun. 149 (2023) 110434.
[120] H. Yang, S. Kou, Recent advances of flexible electrospun nanofibers-based electrodes for electrochemical supercapacitors: a minireview, Int. J. Electrochem. Sci. 14 (2019) 7811–7831.
[121] C. Bavatharani, E. Muthusankar, S.M. Wabaidur, Z.A. Alothman, K.M. Alsheetan, M.m. Al-Anazy, D. Ragupathy, Electrospinning technique for production of polyaniline nanocomposites/nanofibres for multi-functional applications: a review, Synth. Met. 271 (2021) 116609.
[122] B.E. Conway, V. Birss, J. Wojtowicz, The role and utilization of pseudocapacitance for energy storage by supercapacitors, J. Power Sources 66 (1997) 1–14.
[123] S. Bhattacharya, I. Roy, A. Tice, C. Chapman, R. Udangawa, V. Chakrapani, J. L. Plawsky, R.J. Linhardt, High-conductivity and high-capacitance electrospun fibers for supercapacitor applications, ACS Appl. Mater. Interfaces 12 (2020) 19369–19376.
[124] Y. Wang, X. Wu, Y. Xiao, Y. Han, T. Li, Y. Ma, Three dimensional and porous network architecture based on polyaniline hollow nanofibers with high specific capacitance and outstanding cyclic stability for supercapacitor electrode materials, Synth. Met. 299 (2023) 117483.
[125] Y.-E. Miao, W. Fan, D. Chen, T. Liu, High-performance supercapacitors based on hollow polyaniline nanofibers by electrospinning, ACS Appl. Mater. Interfaces 5 (2013) 4423–4428.
[126] A.F. Diaz, K.K. Kanazawa, G.P. Gardini, Electrochemical polymerization of pyrrole, J. Chem. Soc. Chem. Commun. (1979) 635–636.
[127] A. Rudge, I. Raistrick, S. Gottesfeld, J.P. Ferraris, A study of the electrochemical properties of conducting polymers for application in electrochemical capacitors, Electrochim. Acta 39 (1994) 273–287.
[128] A. Eftekhari, L. Li, Y. Yang, Polyaniline supercapacitors, J. Power Sources 347 (2017) 86–107.
[129] J. Liang, S. Su, X. Fang, D. Wang, S. Xu, Electrospun fibrous electrodes with tunable microstructure made of polyaniline/multi-walled carbon nanotube suspension for all-solid-state supercapacitors, Mater. Sci. Eng. B 211 (2016) 61–66.
[130] T. Zheng, X. Wang, Y. Liu, R. Bayaniahangar, H. Li, C. Lu, N. Xu, Z. Yao, Y. Qiao, D. Zhang, P. Pour Shahid Saeed Abadi, Polyaniline-decorated hyaluronic acid-carbon nanotube hybrid microfiber as a flexible supercapacitor electrode material, Carbon 159 (2020) 65–73.
[131] X. Zheng, L. Yao, Y. Qiu, S. Wang, K. Zhang, Core–sheath porous polyaniline nanorods/graphene fiber-shaped supercapacitors with high specific capacitance and rate capability, ACS Applied Energy Materials 2 (2019) 4335–4344.
[132] Z. Li, L. Gong, Research progress on applications of polyaniline (PANI) for electrochemical energy storage and conversion, Materials 13 (2020) 548.
[133] D. Yang, W. Ni, J. Cheng, Z. Wang, C. Li, Y. Zhang, B. Wang, Omnidirectional porous fiber scrolls of polyaniline nanopillars array-N-doped carbon nanofibers for fiber-shaped supercapacitors, Materials Today, Energy 5 (2017) 196–204.
[134] L. Wang, C. Zhang, X. Cao, X. Xu, J. Bai, J. Zhu, R. Li, T. Satoh, Construction of novel coaxial electrospun polyetherimide@polyaniline core-shell fibrous membranes as free-standing flexible electrodes for supercapacitors, J. Power Sources 602 (2024) 234305.
[135] S. Anand, M.W. Ahmad, A.K. Ali Al Saidi, D.-J. Yang, A. Choudhury, Polyaniline nanofiber decorated carbon nanofiber hybrid mat for flexible electrochemical supercapacitor, Mater. Chem. Phys. 254 (2020) 123480.
[136] Y. Cao, H. Zhang, Y. Zhang, Z. Yang, D. Liu, H. Fu, Y. Zhang, M. Liu, Q. Li, Epitaxial nanofiber separator enabling folding-resistant coaxial fiber-supercapacitor module, Energy Storage Materials 49 (2022) 102–110.
[137] T.-L. Chen, Y.A. Elabd, Hybrid-capacitors with polyaniline/carbon electrodes fabricated via simultaneous electrospinning/electrospraying, Electrochim. Acta 229 (2017) 65–72.
[138] Y. Zhang, J.M. Zhang, Q. Hua, Y. Zhao, H. Yin, J. Yuan, Z. Dai, L. Zheng, J. Tang, Synergistically reinforced capacitive performance from a hierarchically structured composite of polyaniline and cellulose-derived highly porous carbons, Mater. Lett. 244 (2019) 62–65.
[139] X. Ni, Y. Jiang, H. Chen, K. Li, H. Chen, Q. Wu, A. Ju, Fabrication of 3D ordered needle-like polyaniline@hollow carbon nanofibers composites for flexible supercapacitors, Chin. Chem. Lett. 32 (2021) 2448–2452.
[140] R.R. Atram, V.M. Bhuse, R.G. Atram, C.-M. Wu, P. Koinkar, S.B. Kondawar, Novel carbon nanofibers/thionickel ferrite/polyaniline (CNF/NiFe2S4/PANI) ternary nanocomposite for high performance supercapacitor, Mater. Chem. Phys. 262 (2021) 124253.
[141] S. Liu, M.-G. Ma, Lignin-derived nitrogen-doped polyacrylonitrile/polyaniline carbon nanofibers by electrospun method for energy storage, Ionics 26 (2020) 4651–4660.
[142] K. Zhang, J. Xu, X. Zhu, L. Lu, X. Duan, D. Hu, L. Dong, H. Sun, Y. Gao, Y. Wu, Poly(3,4-ethylenedioxythiophene) nanorods grown on graphene oxide sheets as electrochemical sensing platform for rutin, J. Electroanal. Chem. 739 (2015) 66–72.
[143] G.P. Pandey, A.C. Rastogi, Solid-state supercapacitors based on pulse polymerized poly(3,4-ethylenedioxythiophene) electrodes and ionic liquid gel polymer electrolyte, J. Electrochem. Soc. 159 (2012) A1664.
[144] J. Yin, Y. Bai, J. Lu, J. Ma, Q. Zhang, W. Hong, T. Jiao, Enhanced mechanical performances and high-conductivity of rGO/PEDOT:PSS/PVA composite fiber films via electrospinning strategy, Colloids Surf. A Physicochem. Eng. Asp. 643 (2022) 128791.
[145] M.A.A. Mohd Abdah, N.H.N. Azman, S. Kulandaivalu, N. Abdul Rahman, A. H. Abdullah, Y. Sulaiman, Potentiostatic deposition of poly(3, 4-ethylenedioxy-thiophene) and manganese oxide on porous functionalised carbon fibers as an advanced electrode for asymmetric supercapacitor, J. Power Sources 444 (2019) 227324.
[146] X. Zhu, X. Han, R. Guo, P. Yuan, L. Dang, Z. Liu, Z. Lei, Vapor-phase polymerization of fibrous PEDOT on carbon fibers film for fast pseudocapacitive energy storage, Appl. Surf. Sci. 597 (2022) 153684.
[147] M.A.A. Mohd Abdah, N.A. Zubair, N.H.N. Azman, Y. Sulaiman, Fabrication of PEDOT coated PVA-GO nanofiber for supercapacitor, Mater. Chem. Phys. 192 (2017) 161–169.
[148] A. Laforgue, All-textile flexible supercapacitors using electrospun poly(3,4-ethylenedioxythiophene) nanofibers, J. Power Sources 196 (2011) 559–564.
[149] M.S. Kolathodi, A. Akbarinejad, C. Tollemache, P. Zhang, J. Travas-Sejdic, Highly stretchable and flexible supercapacitors based on electrospun PEDOT:SSEBS electrodes, J. Mater. Chem. A 10 (2022) 21124–21134.
[150] J. Cárdenas-Martínez, B.L. España-Sánchez, R. Esparza, J.A. Ávila-Niño, Flexible and transparent supercapacitors using electrospun PEDOT:PSS electrodes, Synth. Met. 267 (2020) 116436.
[151] M.A.A. Mohd Abdah, N.H.N. Azman, S. Kulandaivalu, Y. Sulaiman, Asymmetric supercapacitor of functionalised electrospun carbon fibers/poly(3,4-ethylenedioxythiophene)/manganese oxide//activated carbon with superior electrochemical performance, Sci. Rep. 9 (2019) 16782.
[152] P. Wang, H. Zeng, J. Zhu, Q. Gao, Micro-supercapacitors based on ultra-fine PEDOT: PSS fibers prepared via wet-spinning, Chem. Eng. J. 484 (2024) 149676.
[153] M. Skorupa, K. Karoń, E. Marchini, S. Caramori, S. Pluczyk-Małek, K. Krukiewicz, S. Carli, PEDOT:Nafion for highly efficient supercapacitors, ACS Appl. Mater. Interfaces 16 (2024) 23253–23264.
[154] M. Shao, Z. Li, R. Zhang, F. Ning, M. Wei, D.G. Evans, X. Duan, Hierarchical conducting polymer@clay core–shell arrays for flexible all-solid-state supercapacitor devices, Small 11 (2015) 3530–3538.
[155] J. Iqbal, A. Numan, M. Omaish Ansari, R. Jafer, P.R. Jagadish, S. Bashir, P.M. Z. Hasan, A.L. Bilgrami, S. Mohamad, K. Ramesh, S. Ramesh, Cobalt oxide nanograins and silver nanoparticles decorated fibrous polyaniline nanocomposite as battery-type electrode for high performance supercapattery, Polymers 12 (2020) 2816.
[156] S. Liu, K.V. Sankar, A. Kundu, M. Ma, J.-Y. Kwon, S.C. Jun, Honeycomb-like interconnected network of nickel phosphide heteronanoparticles with superior electrochemical performance for supercapacitors, ACS Appl. Mater. Interfaces 9 (2017) 21829–21838.